ISSP Workshop at University of Tokyo
2012/07/10

Electronic structure calculations on liquid-solid interfaces by density functional theory combined with modified Poisson-Boltzmann theory

Ryosuke Jinnouchi[1), 2)] and Alfred B. Anderson[1)]

1) Case Western Reserve University

2) Toyota Central R&D Labs., Inc. (Current affiliation)

Contents: part 1

Introduction:

- Fuel cells technologies.
- What information will be useful (or necessary) for designing electrocatalysts?
- DFT models for inner sphere electron transfer reactions.

Details of our theory:

- Definition of effective PES including solvation contributions.
- Energy minimization by variational principles.
- Forces acting on atoms.
- Some guidelines for choice of the

Some applications in CWRU:

- Aqueous and surface redox potentials.
- PZC, water flip-flop and the role of the dielectric medium.

Conclusion:

Introduction

Introduction: fuel cells technologies

Objectives

- By 2015, a fuel cell system for portable power (<250 W) with an energy density of 900 Wh/L.
- By 2017, a 60% peak-efficient, 5,000 hour durable, direct hydrogen fuel cell power system for transportation at a cost of $30/kW.
- By 2020, distributed generation and micro-CHP fuel cell systems (5 kW) operating on natural gas or LPG that achieve 45% electrical efficiency and 60,000 hours durability at an equipment cost of $1500/kW.
- By 2020, medium-scale CHP fuel cell systems (100 kW–3 MW) with 50% electrical efficiency, 90% CHP efficiency, and 80,000 hours durability at an installed cost of $1,500/kW for operation on natural gas, and $2,100/kW when configured for operation on biogas.
- By 2020, APU fuel cell systems (1–10 kW) with a specific power of 45 W/kg and a power density of 40W/L at a cost of $1000/kW.

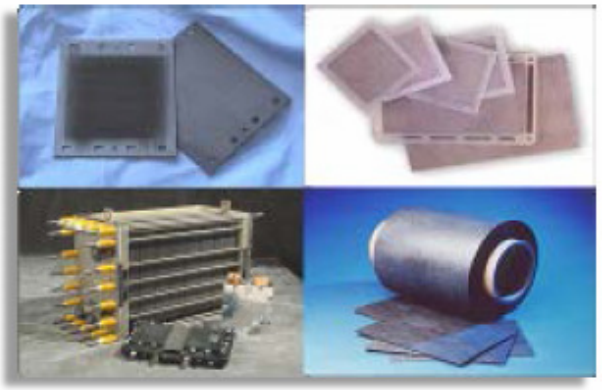

Taken from a presentation by Dr. Papageorgopoulos 2012 Annual Merit Review and Peer Evaluation Meeting of DOE.

Introduction: fuel cells vs. battery

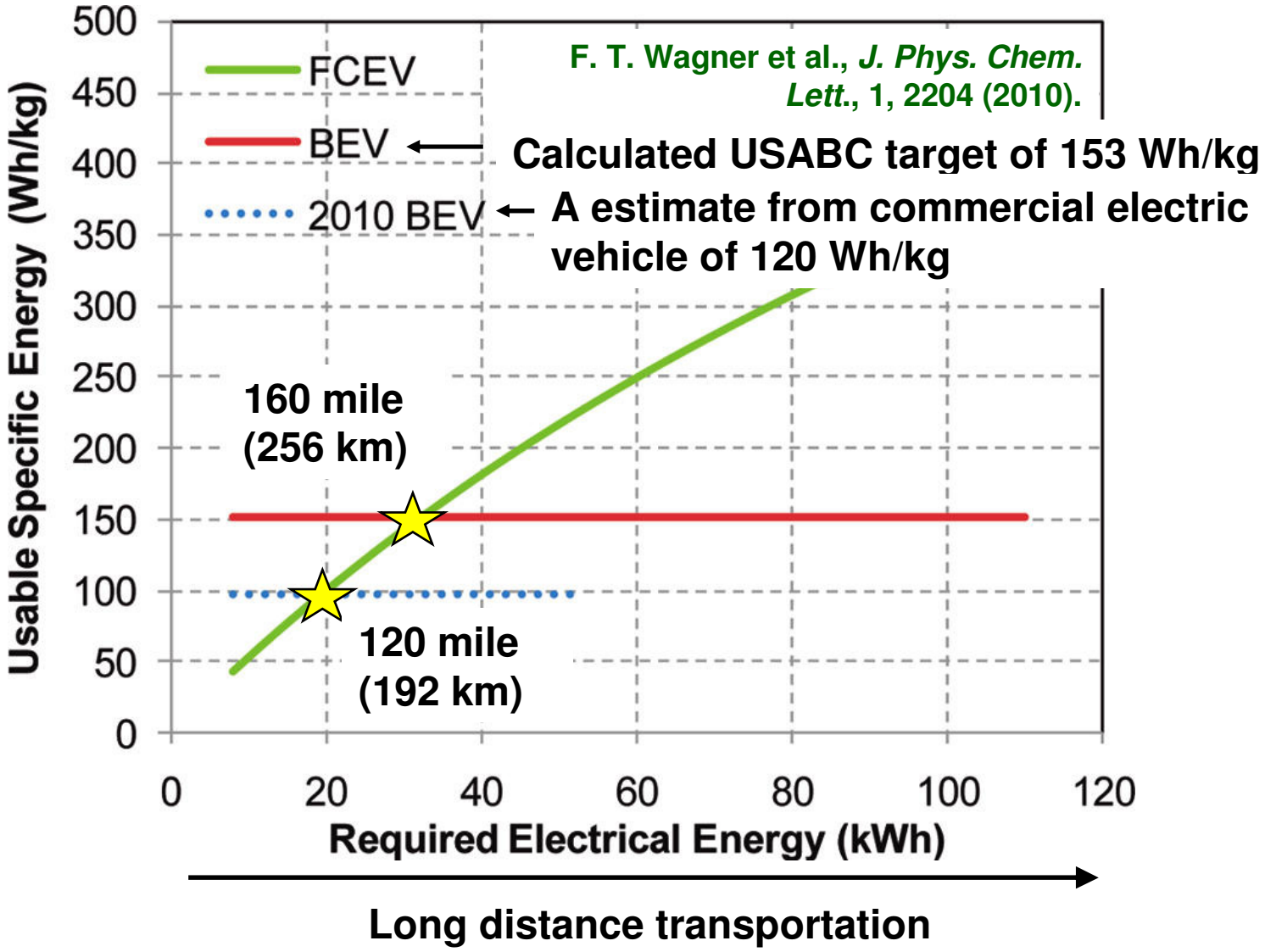

Battery for short distance and fuel cells for long distance.
Fuel cells and battery are not competitive but cooperative.

Introduction: Electrochemistry in fuel cells

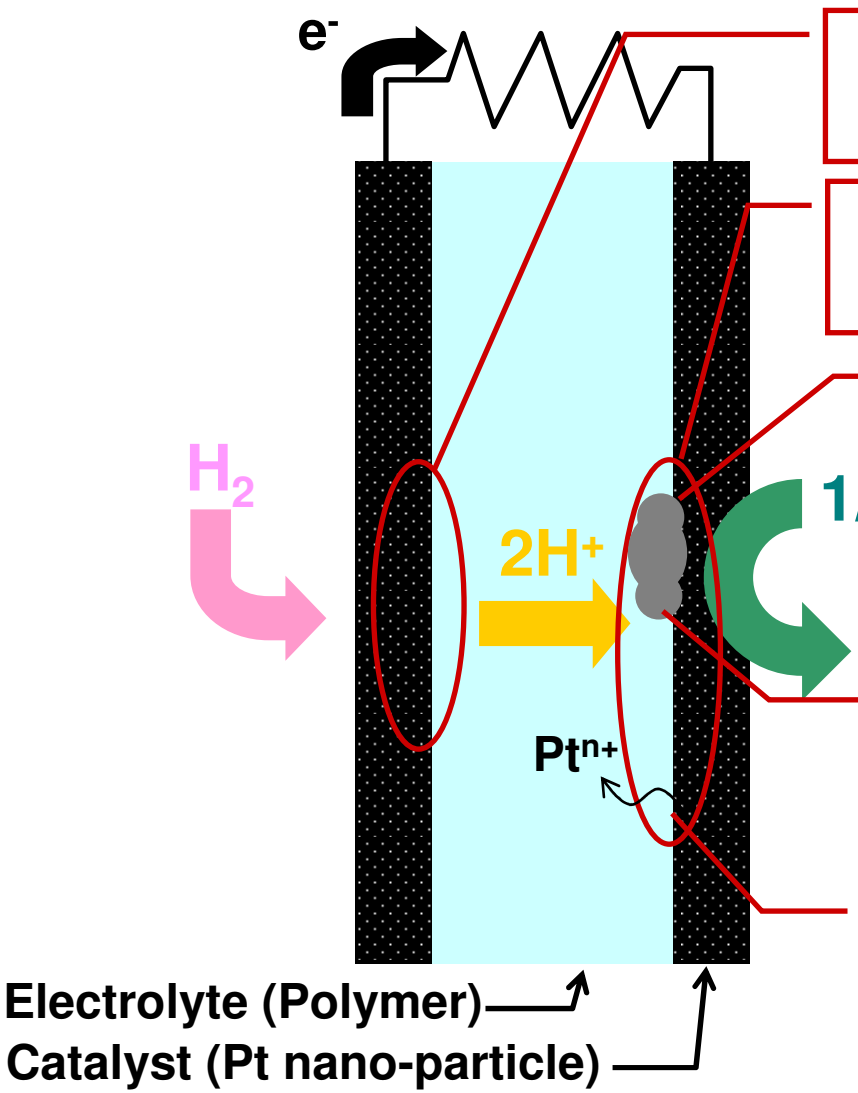

Hydrogen oxidation reaction (HOR)

$H_2 \rightarrow 2H^+(aq) + 2e^-$

Oxygen reduction reaction (ORR)

$1/2\ O_2(g) + 2H^+(aq) + 2e^- \rightarrow H_2O(aq)$

Oxidation of Pt and site blocking

$Pt + H_2O(aq) \rightarrow OH\text{-}Pt + H^+(aq) + e^-$

Specific adsorption and site blocking

$R\text{-}SO_3^- + Pt \rightarrow R\text{-}[SO_3\text{-}Pt]^{-(1-\delta)} + \delta e^-$

Dissolution of Pt

$Pt \rightarrow Pt^{n+}(aq) + ne^-$

Introduction: higher mass activity for ORR

$$O_2(g) + 4H^+(aq) + 4e^- \rightarrow 2H_2O(aq)$$

Current status:	**0.3 A·mg^{-1} (for Pt/C)**
DOE target:	**0.44 A·mg^{-1}**
NEDO project target:	**3.00 A·mg^{-1}**

State-of-the-art catalysts: **Pt alloys and core-shells**

Introduction: more durable electrocatalysts

$$Pt \rightarrow Pt^{2+}(aq) + 2e^-$$

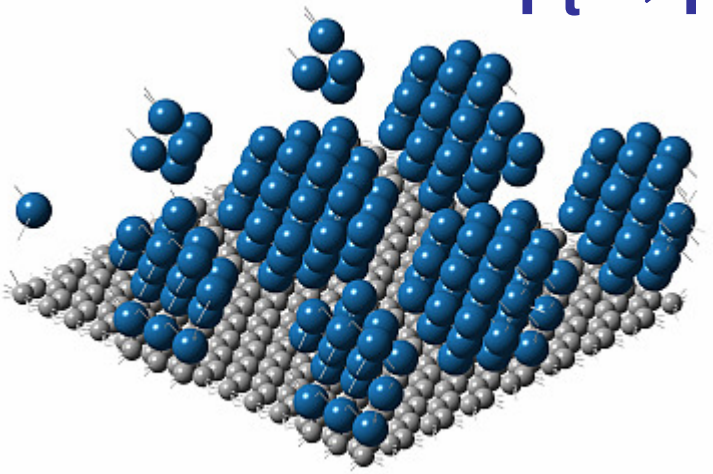

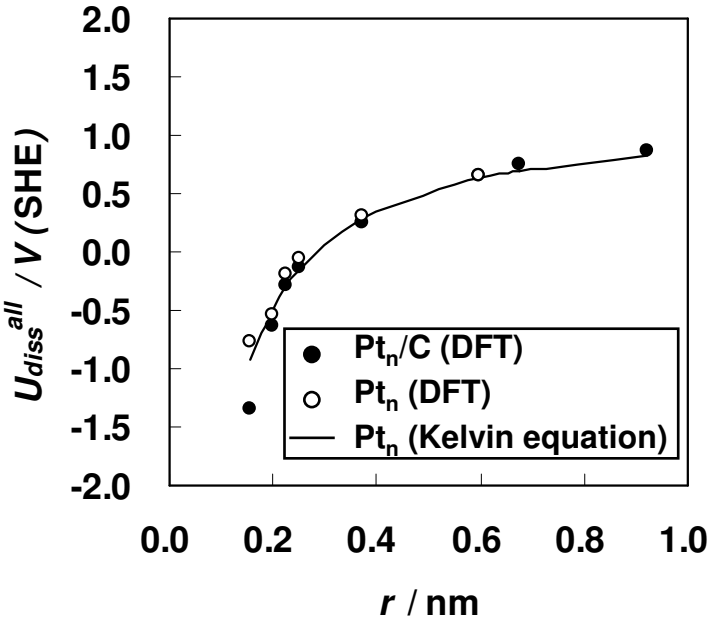

Jinnouchi et al., *J. Phys. Chem. C,* 114, 17557 (2010).

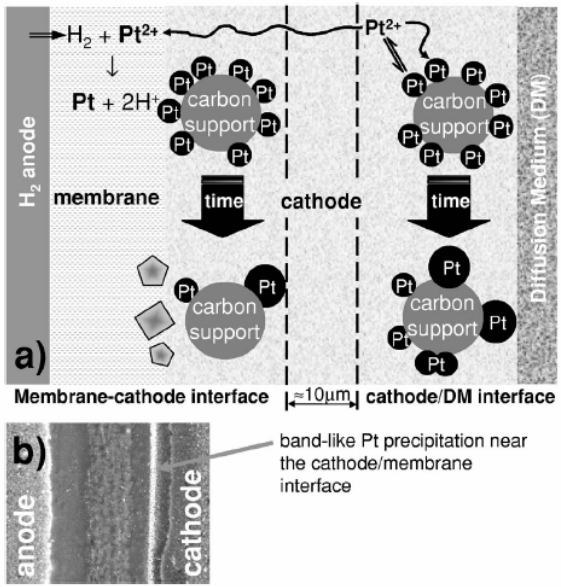

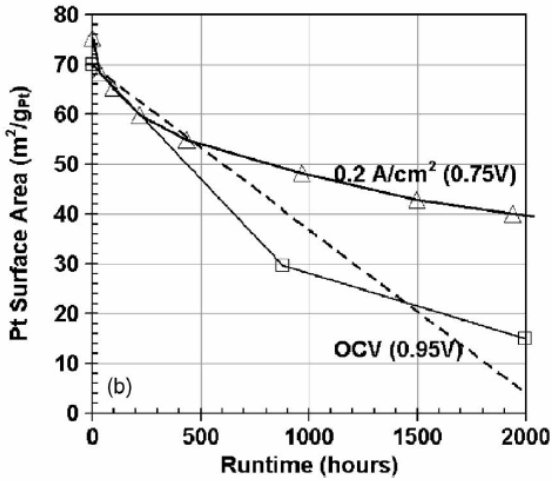

Ferreira et al., *J. Electrochem. Soc.*, 152, A2256 (2005).

Introduction: poisoning by specific adsorptions

$$R\text{-}SO_3^-(aq) \rightarrow R\text{-}SO_3^{-(1-\delta)}(ads) + \delta e^-$$

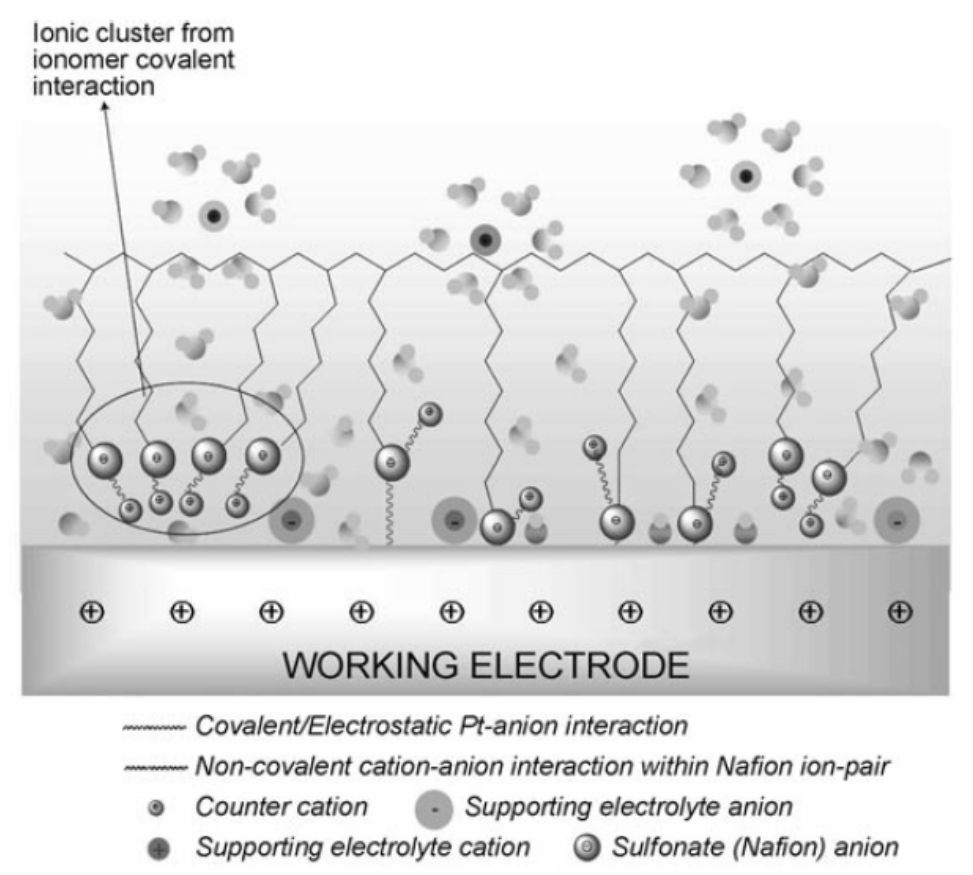

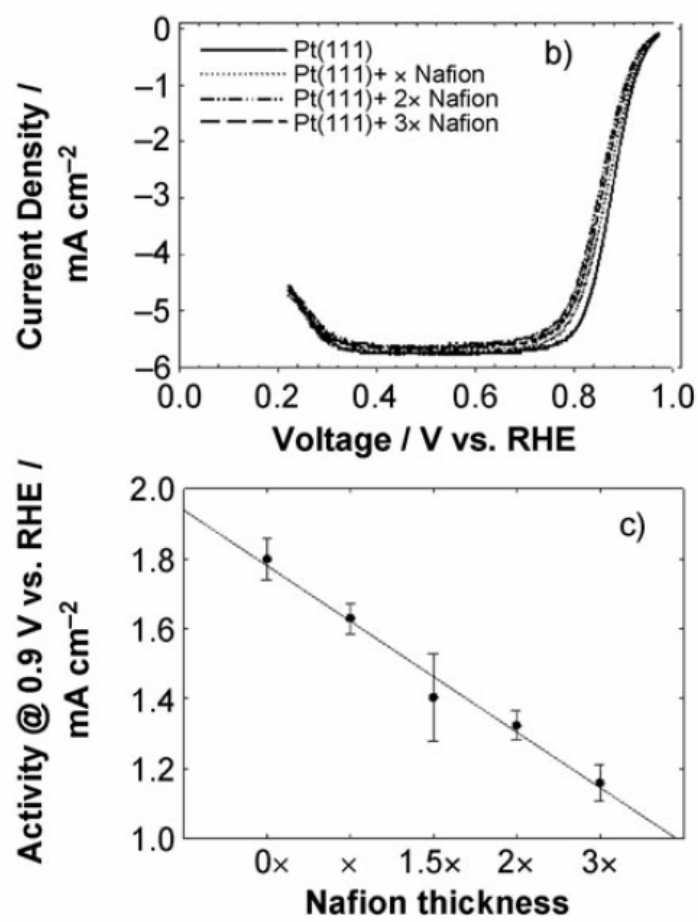

Subbaraman et al., *ChemPhysChem*, 11, 2825 (2010).

Introduction: electrode reactions for catalyst fabrications

Fabrications of core-shell catalysts using Cu-UPD.

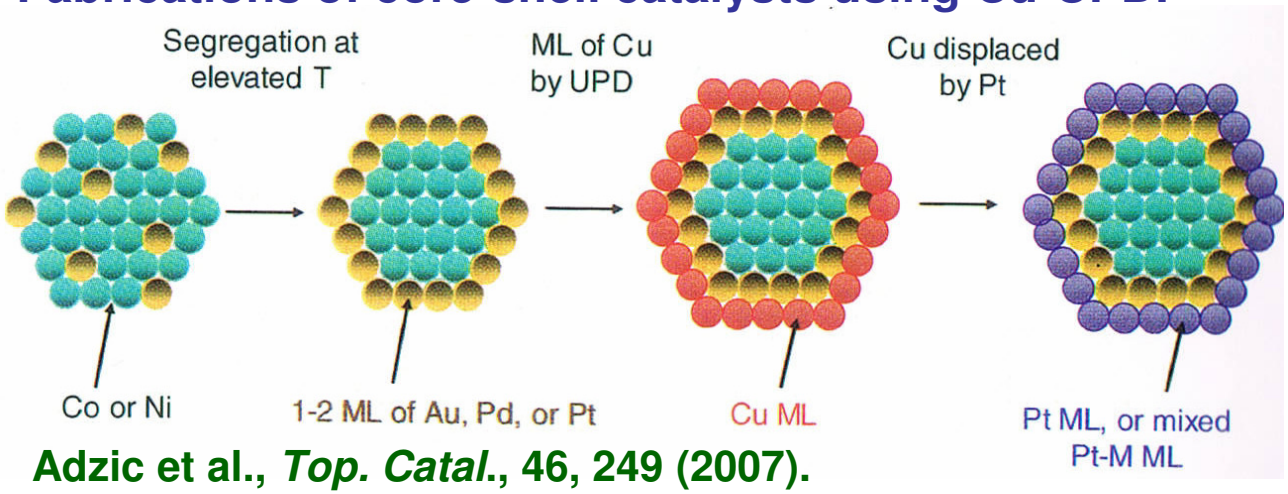

Adzic et al., *Top. Catal.*, 46, 249 (2007).

CO annealing for removing adatoms and kinks.

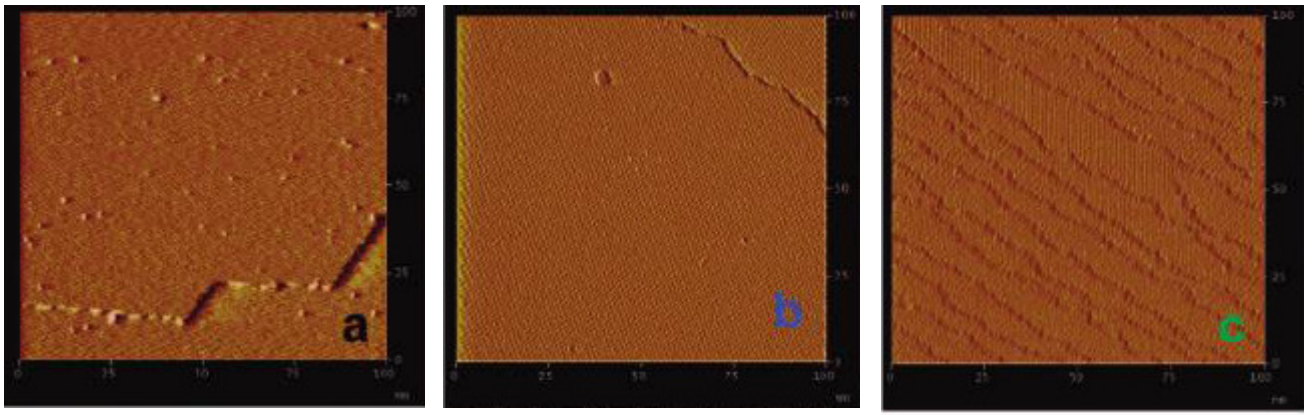

Strmcnik et al., *J. Am. Chem. Soc.*, 130, 15332 (2008).

Introduction: Electrochemistry in fuel cells

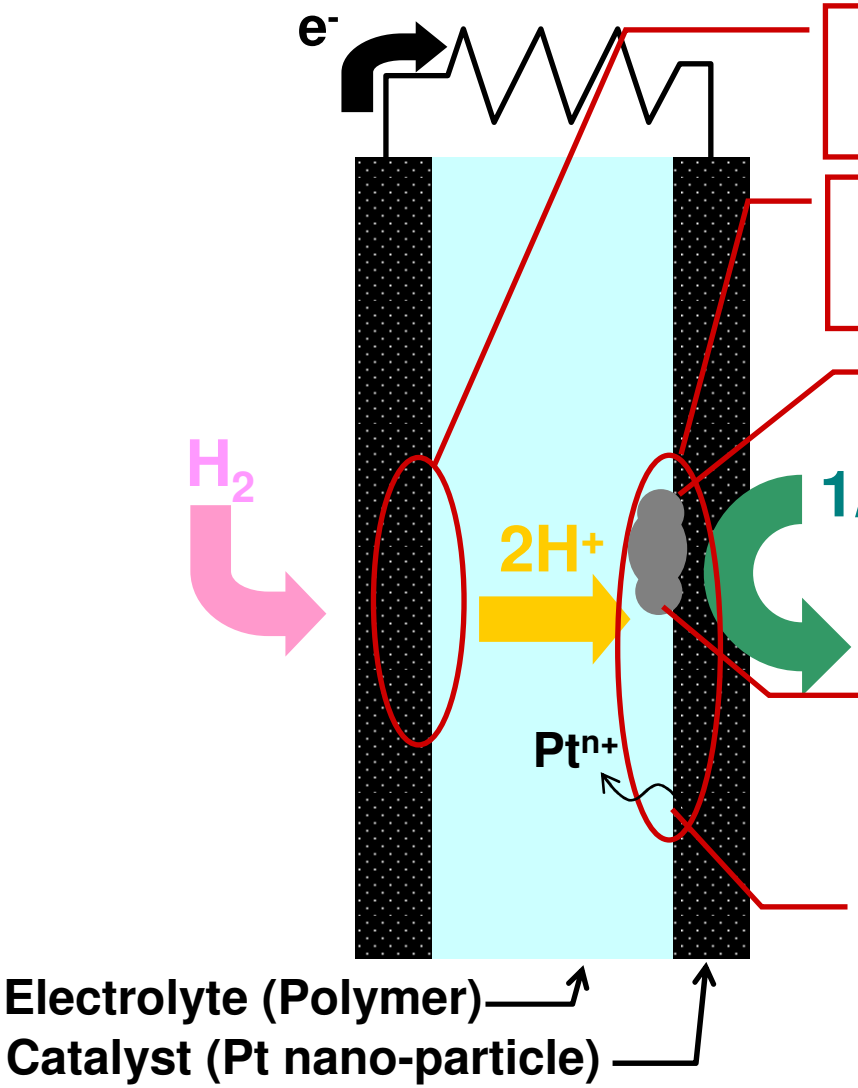

Hydrogen oxidation reaction (HOR)

$H_2 \rightarrow 2H^+(aq) + 2e^-$

Oxygen reduction reaction (ORR)

$1/2\ O_2(g) + 2H^+(aq) + 2e^- \rightarrow H_2O(aq)$

Oxidation of Pt and site blocking

$Pt + H_2O(aq) \rightarrow OH\text{-}Pt + H^+(aq) + e^-$

Specific adsorption and site blocking

$R\text{-}SO_3^- + Pt \rightarrow R\text{-}[SO_3\text{-}Pt]^{-(1-\delta)} + \delta e^-$

Dissolution of Pt

$Pt \rightarrow Pt^{n+}(aq) + ne^-$

Accurate and practically useful atomic-scale theories to predict thermodynamics and kinetics of electrocatalysis are necessary.

Introduction: what information is useful or necessary?

R. B. Getman et al. J. Phys. Chem. C, 112, 2008, 9559.

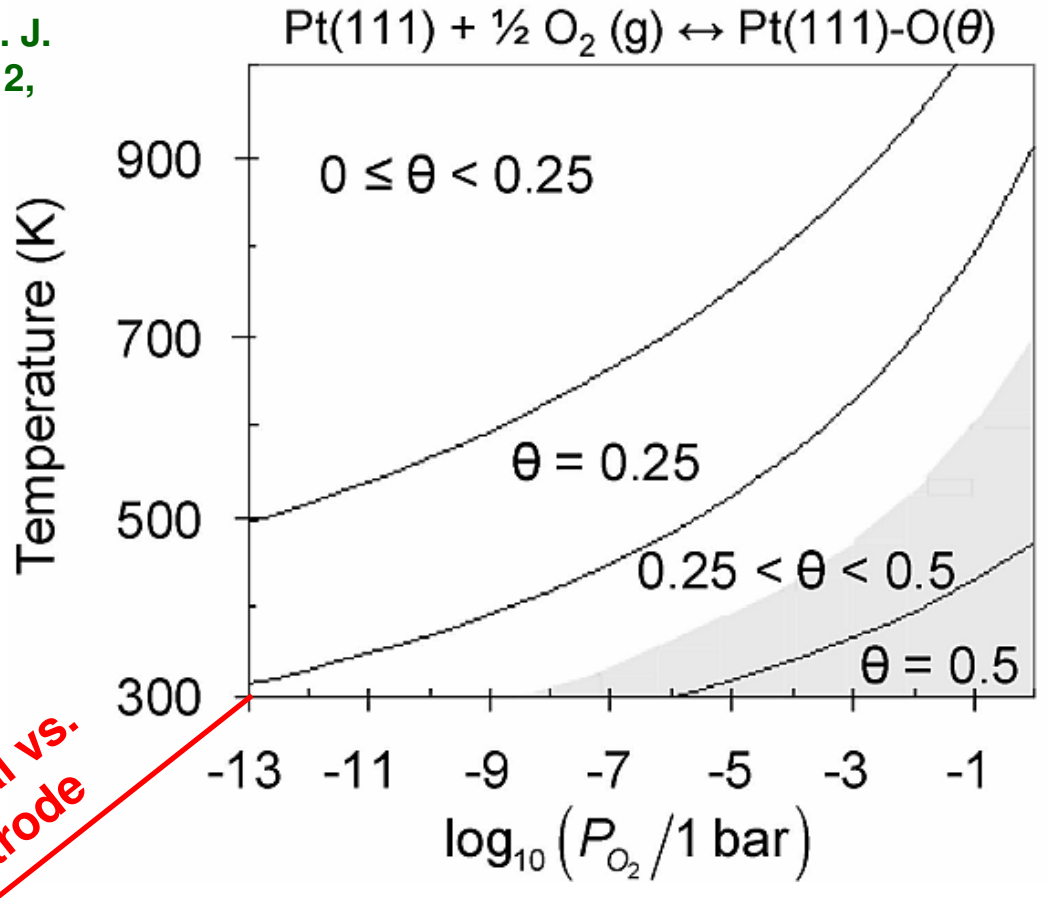

The most important thermodynamic parameter, that is the electrode potential *U* , is introduced in electrochemistry.

Surface state and kinetics drastically changes by just a 10 – 100 mV change in *U*.

Introduction: what information is useful or necessary?

Electrochemists including practical engineers always want to know how the surface state changes with the change in the electrode potential.

The theoretical methodology, which can give such information comparable with experiments by a practical computational time, is useful or necessary.

Introduction: reactions at electrified interfaces

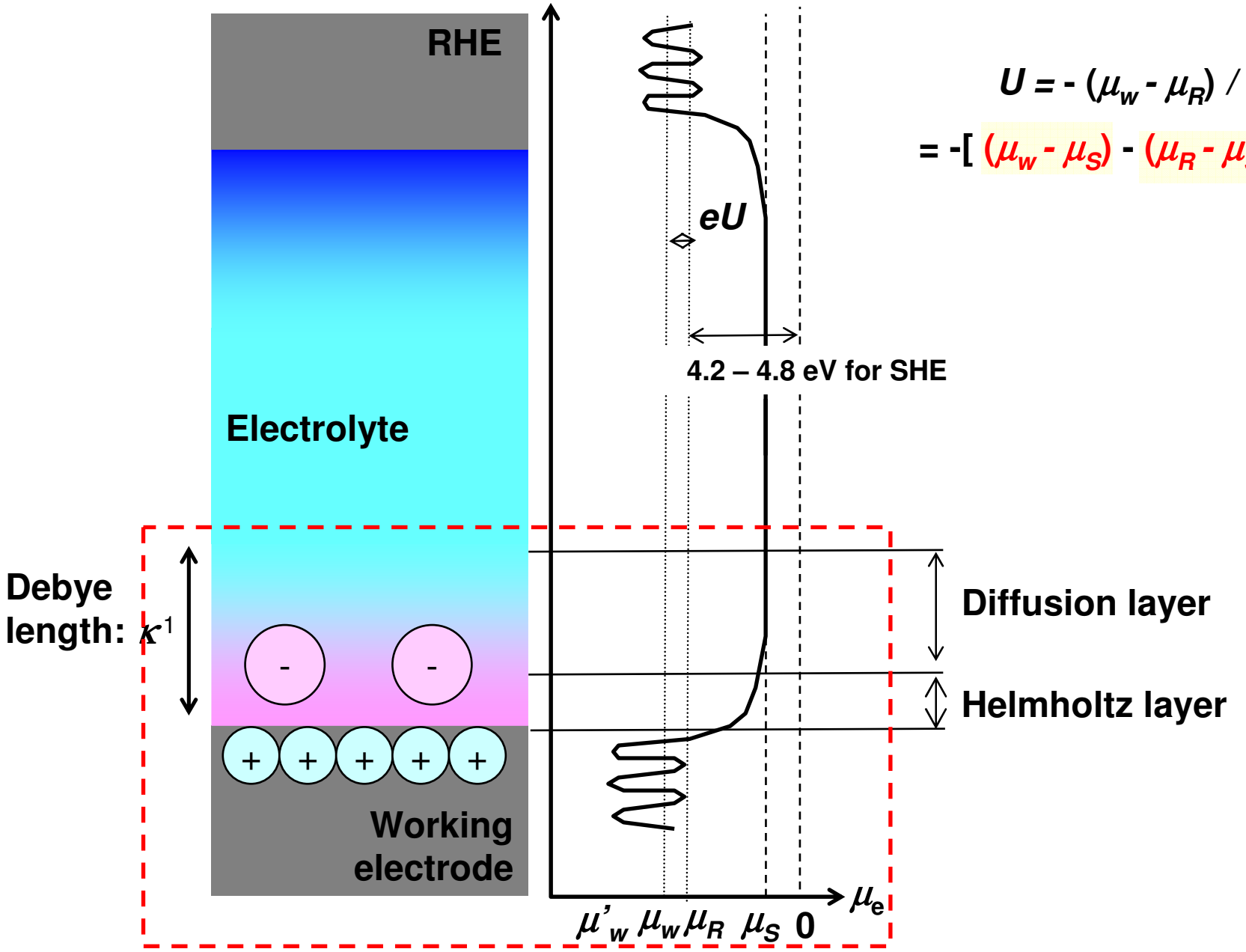

$$U = -(\mu_w - \mu_R)/e$$

$$= -[(\mu_w - \mu_S) - (\mu_R - \mu_S)]/e$$

Introduction: Local reaction center model

The first practically applicable theory predicting activation energies of electrode reactions.
Locating transition states at intersections of multi-potential energy surfaces.

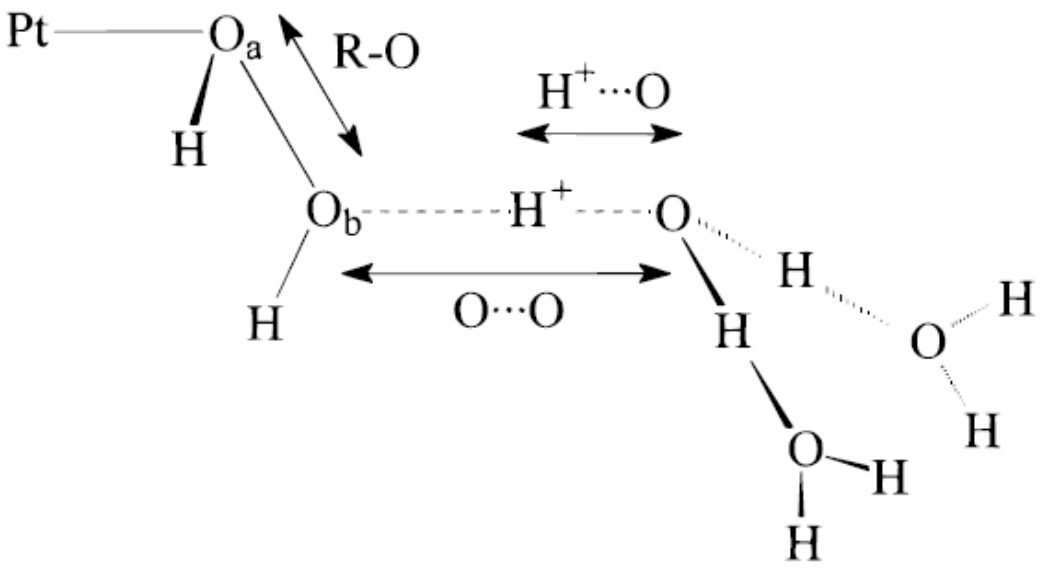

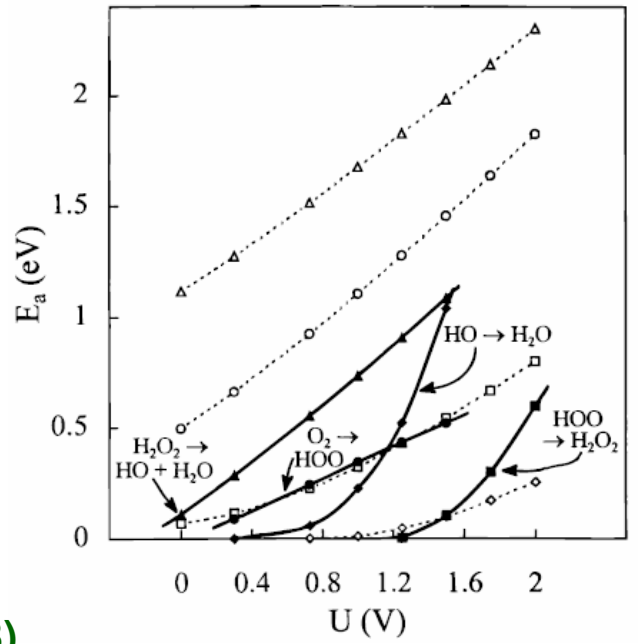

Anderson and Kang, *J. Phys. Chem. A*, 102, 5993 (1998).
Anderson and Albu, *J. Am. Chem. Soc.*, 121, 11855 (1999).
Anderson and Albu, J. Electrochem. Soc., 147, 4229 (2000).
...
Zhang and Anderson, *J. Phys. Chem. C*, 113, 3197 (2009).

Introduction: DFT calculations using neutral slabs (1)

Methodologies using neutral slabs were suggested by professor Anderson's group and professor Nørskov's group in 2004.
It is still one of the most useful methodologies to predict thermodynamics of electrode reactions quantitatively.

Linear Gibbs energy relationship for predicting reversible potential forming OH(ads)

Roques and Anderson, *J. Electrochem. Soc.*, 151, E85 (2004).

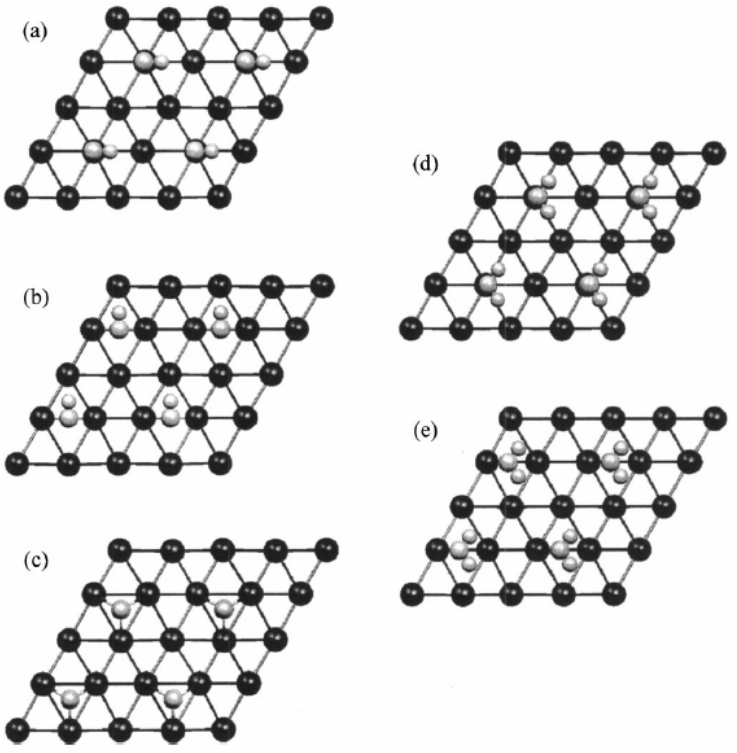

Predicting volcano plot of ORR.

Nørskov et al., *J. Phys. Chem. B*, 108, 17886 (2004).

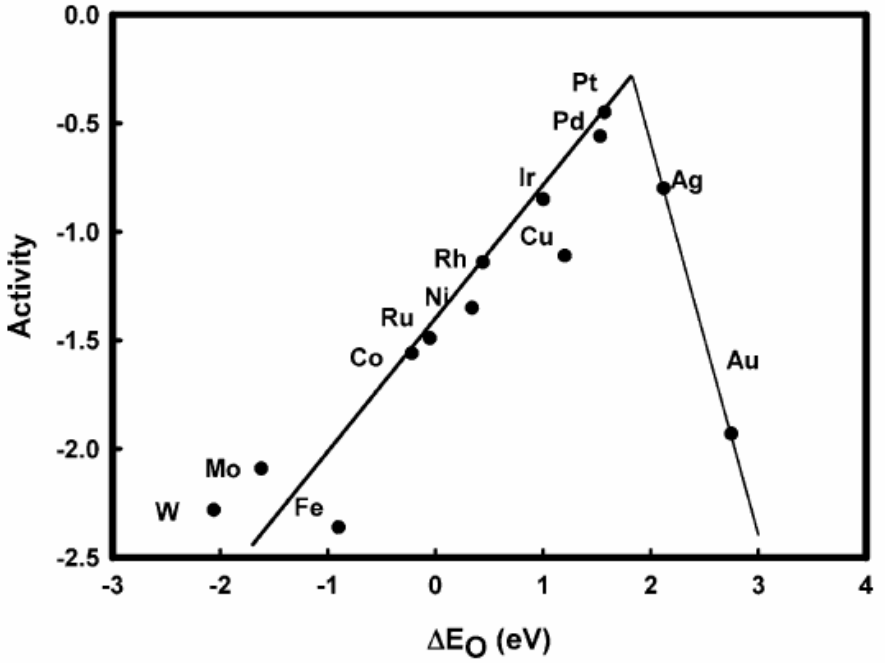

Introduction: DFT calculations using neutral slabs (2)

A → B

$$\frac{1}{e}\frac{\partial \Delta G}{\partial U} = -\{n_B(U) - n_A(U)\} = \gamma(U)$$

- $\gamma(U)$: Electrosorption valency value
- $n_A(U)$: Number of electrons for state A
- $n_B(U)$: Number of electrons for state B

For example, see “Trasatti and Parsons, *J. Electroanal. Chem.*, 1986, 205, 359” or “W. Schmickler and E. Santos, *Interfacial Electrochemistry*, *2nd Edition*, Springer, 1996”.

The equation can be also derived from DFT formalism as shown later in this presentation.

Introduction: DFT calculations using neutral slabs (3)

A → B

$$\frac{1}{e}\frac{\partial \Delta G}{\partial U} = -\{n_B(U) - n_A(U)\} \cong -(n_B - n_A)$$

← Approximation and assumption on the charge transferred by the reaction.

$$\Delta G \cong \Delta G_0 - e(n_B - n_A)U$$

← ΔG_0 is ΔG at U = 0 V.

$$\Delta G_0 \cong \Delta E + \Delta ZPE - T\Delta S$$

← Approximation on ΔG_0 using a difference in the Gibbs free energies given by DFT calculations on neutral slabs.

$$U_{\text{rev}} \cong \frac{\Delta E + \Delta ZPE - T\Delta S}{e(n_B - n_A)}$$

Introduction: DFT calculations using neutral slabs (4)

The method is useful but has limitations.

(i) The method cannot predict the charge transferred by the electrode reaction. Hence, the method cannot predict electrochemical properties related to the charge transfers, such as capacitances and electrosorption valency values.

(ii) The method cannot locate transition states. Hence, it cannot predict the activation energies.

(iii) When the adsorbate has a large dipole and interacts with the electric field by the electric double layer, the method will cause large errors.

A methodology which explicitly handle the charged slabs is necessary to overcome the problems.

Introduction: DFT calculations on charged slabs

A first DFT calculation on charged slab.

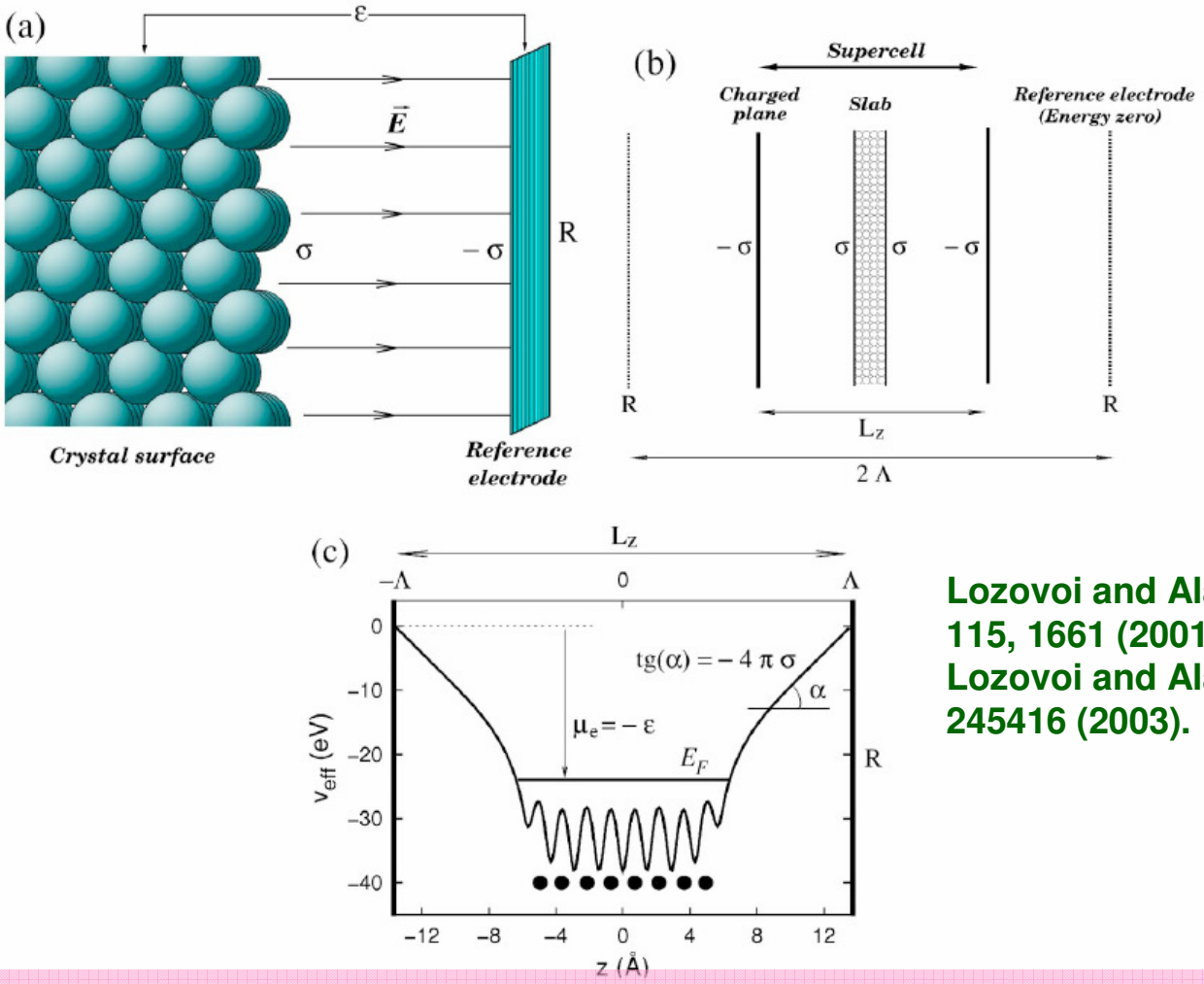

Lozovoi and Alavi, *J. Chem. Phys.*, 115, 1661 (2001).
Lozovoi and Alavi, *Phys. Rev. B*, 68, 245416 (2003).

Slabs are placed in vacuum, and therefore, the system is far from the solid-liquid interface.

Introduction: double reference method

$$\phi_q(f) = \phi'_q(f) - \phi'_q(w) + \phi_0(w).$$

$$U_q/\mathrm{V} = -4.8 - \phi_q(f)/\mathrm{eV}.$$

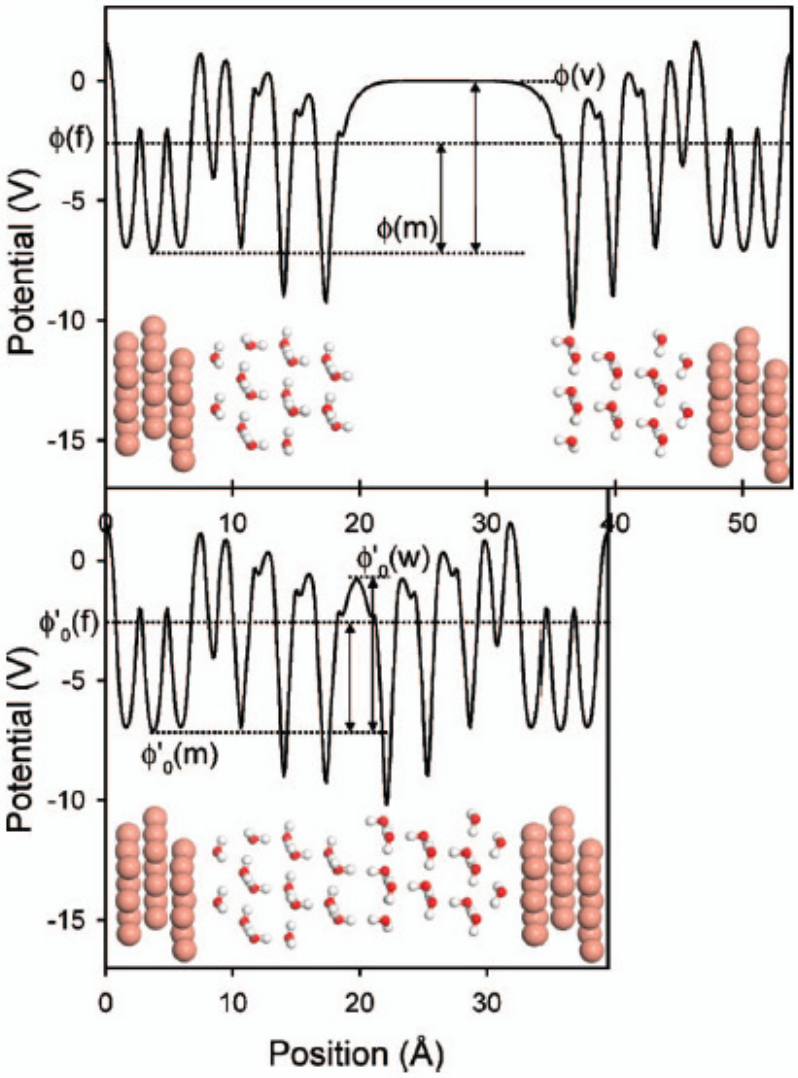

Taylor et al., *Phys. Rev. B*, 73, 165402 (2006).

(i) Problems related to the background charge: Too large screening, too thin double layer, etc.

(ii) Problems related to the ice like water layer: Too many local minima, large noises hindering the small energy differences by the reaction, etc.

More accurate description of ion distribution is necessary.

Introduction: Effective screening medium

A method combining DFT with a modified Poisson-Boltzmann theory (MPB).

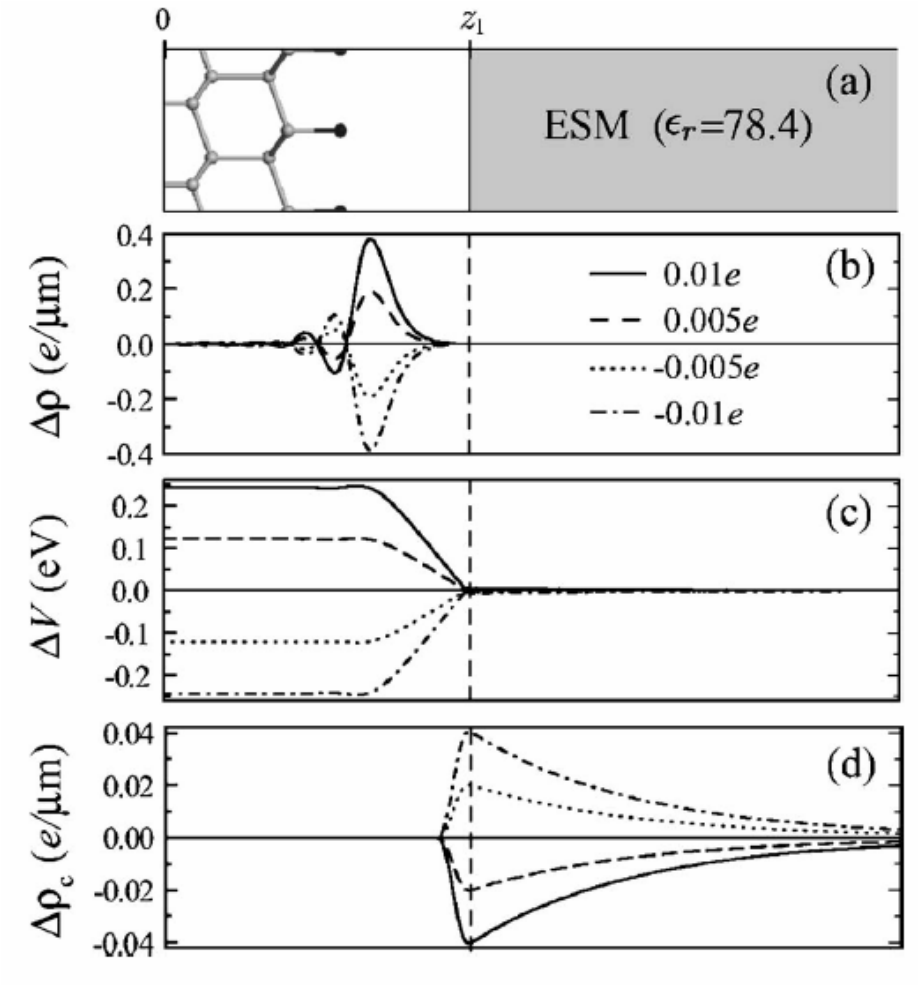

This version of the ESM seems to be very good.

However, details of the definitions for the DFT-MPB interface are necessary as PCM, COSMO or SM*x* needed those when it was developed from the Born model.

Otani and Sugino, *Phys. Rev. B*, 73, 115407 (2006).

Objective

Making a more accurate, practically useful and robust computational method for liquid-solid interfaces by combining the density functional theory and a modified Poisson-Boltzmann theory.

Method

Method: combining DFT with MPB by PCM

Otani and Sugino, *Phys. Rev. B*, 73, 115407 (2006).

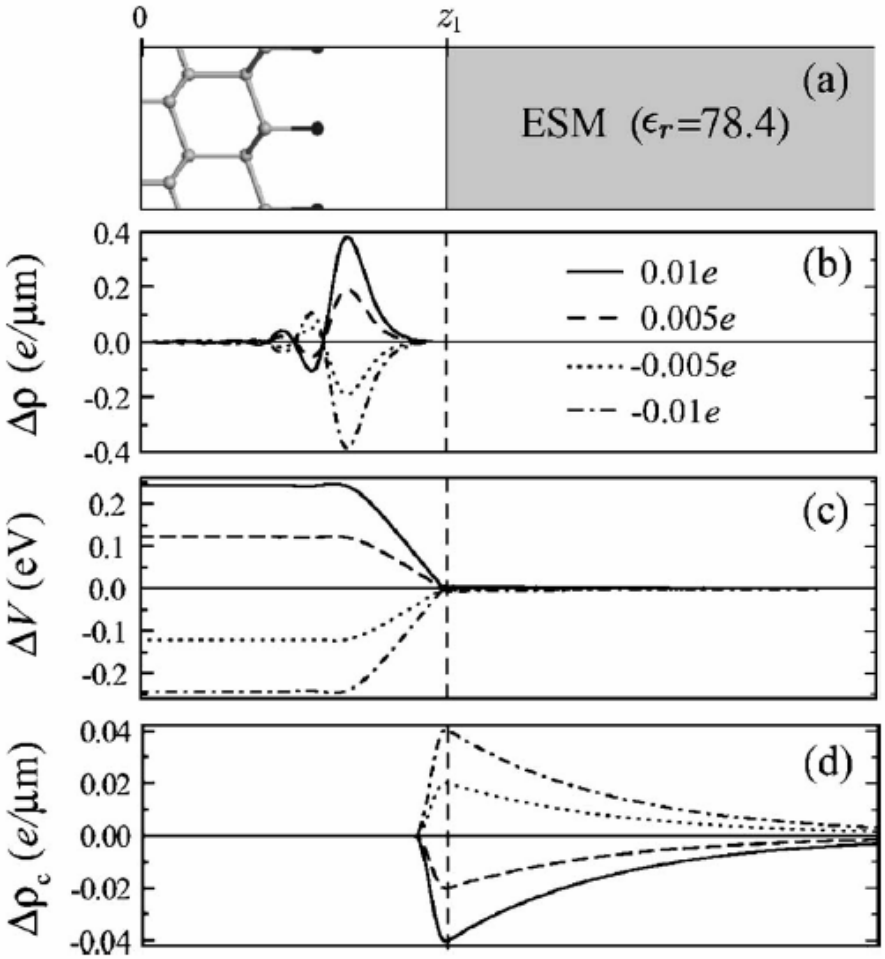

J. Fattebert, et al., *J. Comp. Chem.*, 93, 139 (2003)
D. A. Scherlisa, et al., *J. Chem. Phys.*, 124, 074103, (2006).

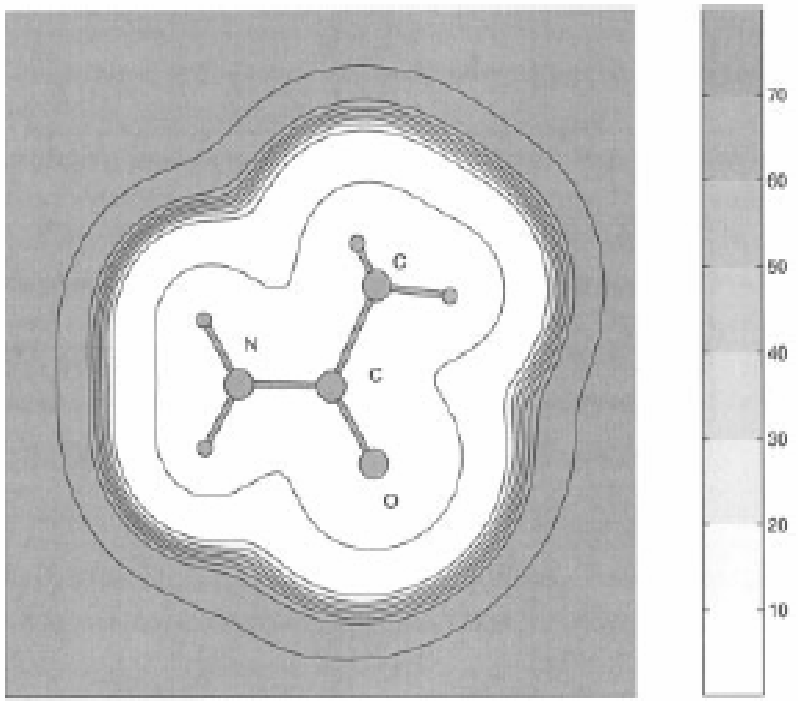

Similarly to PCM for molecular theory, a smooth and adaptive dielectric permittivity will be useful for connecting DFT and MPB.

Method: problems in the combination

(i) Definition of energy functional which makes us possible to exclude ion in MPB region from DFT region.

(ii) Definition of the dielectric permittivity appropriate for slabs (The PCM calculations for slabs were not done at that time).

(iii) A robust numerical method to minimize the energy functional for slab sytems.

Method: PES for atoms

$$V(\{\mathbf{R}_\alpha\}) = E(\{\mathbf{R}_\alpha\}) - \mu_e N_e - \mu_+ N_+ - \mu_- N_-$$

Jinnouchi and Anderson, *PRB*, 77, 245417 (2008).

$$E(\{\mathbf{R}_\alpha\}) = -K + E_{xc} + E_{es} - T_e S_e + G_{ss,nes} + G_{is,nes} - TS_i$$

$$K = \sum_n f_n \int d\mathbf{r}\, \psi_n^*(\mathbf{r}) \left(-\frac{1}{2}\nabla^2 \right) \psi_n(\mathbf{r})$$ ← Kinetic energy of electrons

$$E_{xc} = E_{xc}[\rho_\uparrow, \rho_\downarrow] = \int d\mathbf{r} f_{xc}(\rho_\uparrow, \rho_\downarrow, \nabla\rho_\uparrow, \nabla\rho_\downarrow)$$ ← Exchange-correlation energy of electrons

$$E_{es} = \int d\mathbf{r}[\rho_\uparrow(\mathbf{r}) + \rho_\downarrow(\mathbf{r}) + \rho_c(\mathbf{r}) + \rho_+(\mathbf{r}) + \rho_-(\mathbf{r})]\phi(\mathbf{r}) - \int d\mathbf{r} \frac{\varepsilon(\mathbf{r})}{8\pi} |\nabla\phi(\mathbf{r})|^2$$ ← Electrostatic energy of whole system

$$G_{ss,cav} = \gamma_b S$$ ← Cavitation free energy describing non-electrostatic interaction between solute and solvent.

$$G_{ss,dr} + G_{ss,rep} = \sum_\alpha (a_\alpha S_\alpha + b_\alpha)$$ ← Dispersion and repulsion free energy describing non-electrostatic interaction between solute and solvent.

$$G_{is,nel} = \int d\mathbf{r}(|\rho_-(\mathbf{r})| + |\rho_+(\mathbf{r})|)\phi_{rep}(\mathbf{r})$$ ← Non-electrostatic repulsive interaction describint non-electrostatic interaction between solute and continuum ions.

$$S_i = -\frac{k_B}{a^3} \int d\mathbf{r}[|\rho_+(\mathbf{r})|a^3 \ln(|\rho_+(\mathbf{r})|a^3) + |\rho_-(\mathbf{r})|a^3 \ln(|\rho_-(\mathbf{r})|a^3)$$ ← Entropy of continuum electrolyte.

$$+ (1 - |\rho_+(\mathbf{r})|a^3 - |\rho_-(\mathbf{r})|a^3) \ln(1 - |\rho_+(\mathbf{r})|a^3 - |\rho_-(\mathbf{r})|a^3)$$

$$N_\pm = \int \rho_\pm(\mathbf{r}) d\mathbf{r} \mu_\pm = k_B T \ln \frac{c_b a^3}{1 - 2c_b a^3}$$ ← Chemical potentials of continuum ions.

Method: electrostatic energy and dielectric permittivity (1)

Charges by electrons in the DFT region

Charges by nuclei in the DFT region

Charges by ion in the MPB region

$$E_{es} = \int d\mathbf{r}\left[\rho_{\uparrow}(\mathbf{r}) + \rho_{\downarrow}(\mathbf{r}) + \rho_{c}(\mathbf{r}) + \rho_{+}(\mathbf{r}) + \rho_{-}(\mathbf{r})\right]\phi(\mathbf{r}) - \int d\mathbf{r}\,\frac{\varepsilon(\mathbf{r})}{8\pi}\left|\nabla\phi(\mathbf{r})\right|^{2}$$

Position-dependent dielectric permittivity

Original definition

J. Fattebert, et al., *J. Comp. Chem.*, 93, 139 (2003)

$$\varepsilon(\mathbf{r}) = 1 + \frac{\varepsilon_b - 1}{2}\left[1 + \frac{1 - \left\{\frac{\rho(\mathbf{r})}{\rho_0}\right\}^{2\beta}}{1 + \left\{\frac{\rho(\mathbf{r})}{\rho_0}\right\}^{2\beta}}\right]$$

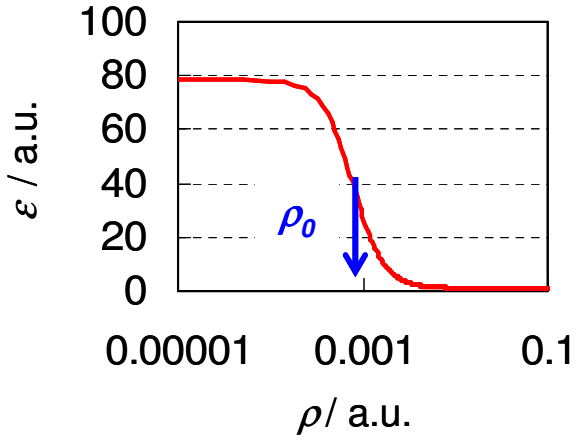

Our new definition

Jinnouchi and Anderson, *PRB*, 77, 245417 (2008).

Summation of ground-state atomic electron densities

$$\varepsilon(\mathbf{r}) = 1 + \frac{\varepsilon_b(\mathbf{r}) - 1}{2}\left[1 + \frac{1 - \left\{\frac{\rho_{AE}(\mathbf{r})}{\rho_0}\right\}^{2\beta}}{1 + \left\{\frac{\rho_{AE}(\mathbf{r})}{\rho_0}\right\}^{2\beta}}\right]$$

Position-dependent bulk dielectric permittivity

Method: electrostatic energy and dielectric permittivity (2)

Jinnouchi and Anderson, *PRB*, 77, 245417 (2008).

Summation of ground-state atomic electron densities:

(i) It is smoother than the molecular electron density. Hence, it does not need fine grids for solving the Poisson equation.

(ii) Modification does not change the accuracy at all.

The same idea is utilized in later implementations described in

Sánchez et al. in *J. Chem. Phys.*, 131, 174108 (2009),
Fang and Liu in *J. Am. Chem. Soc.*, 132, 18214 (2010),
Fang, Wei and Liu, Catal. Today, published.

$$\varepsilon(\mathbf{r}) = 1 + \frac{\varepsilon_b(\mathbf{r}) - 1}{2}\left[1 + \frac{1 - \left\{\frac{\rho_{AE}(\mathbf{r})}{\rho_0}\right\}^{2\beta}}{1 + \left\{\frac{\rho_{AE}(\mathbf{r})}{\rho_0}\right\}^{2\beta}}\right]$$

Position-dependent bulk dielectric permittivity:

It makes us possible to define more appropriate definition of ε for slabs.

$$\varepsilon_\infty(\mathbf{r}) = \begin{cases} \varepsilon_b \\ -\dfrac{\varepsilon_b - 1}{2}\left[1 - \mathrm{erf}\left(\dfrac{z - z_0}{\Delta_z}\right)\right] + \varepsilon_b \end{cases}$$

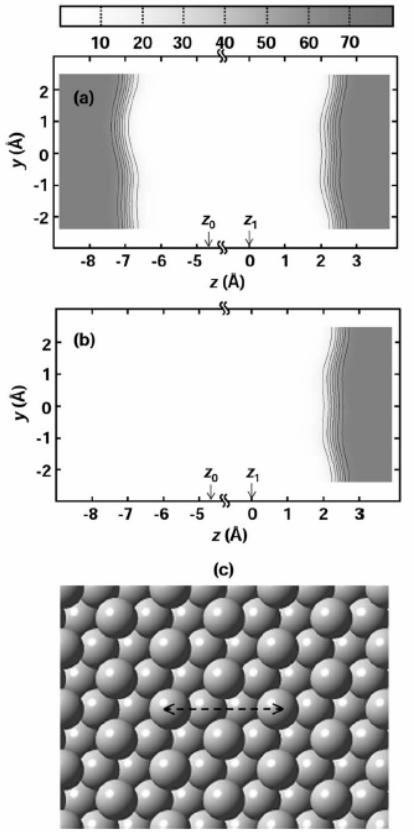

Method: cavitation free energy

Original definition

D. A. Scherlisa, et al., *J. Chem. Phys.*, 124, 074103, (2006).

$$G_{ss,cav} = \gamma_b S, \quad S = \int s[\rho, \nabla\rho] d\mathbf{r}$$

$$s[\rho,\nabla\rho] = \left[\vartheta_{\rho_0 - \frac{1}{2}\Delta}(\rho) - \vartheta_{\rho_0 + \frac{1}{2}\Delta}(\rho) \right] \frac{|\nabla\rho|}{\Delta} = \left. \frac{\partial\vartheta}{\partial\rho_0} \right|_{\rho} |\nabla\rho|$$

$$\vartheta_{\rho_0}(\rho) = \frac{1}{2}\left[\frac{\left(\frac{\rho}{\rho_0}\right)^{2\beta} - 1}{\left(\frac{\rho}{\rho_0}\right)^{2\beta} + 1} + 1 \right]$$

Our new definition

Jinnouchi and Anderson, *PRB*, 77, 245417 (2008).

$$G_{ss,cav} = \gamma_b(\mathbf{r}) S, \quad S = \int s[\rho, \nabla\rho] d\mathbf{r}$$

$$s[\rho_{AE},\nabla\rho_{AE}] = \left[\vartheta_{\rho_0 - \frac{1}{2}\Delta}(\rho_{AE}) - \vartheta_{\rho_0 + \frac{1}{2}\Delta}(\rho_{AE}) \right] \frac{|\nabla\rho_{AE}|}{\Delta} = \left. \frac{\partial\vartheta}{\partial\rho_0} \right|_{\rho} |\nabla\rho_{AE}|$$

$$\vartheta_{\rho_0}(\rho_{AE}) = \frac{1}{2}\left[\frac{\left(\frac{\rho_{AE}}{\rho_0}\right)^{2\beta} - 1}{\left(\frac{\rho_{AE}}{\rho_0}\right)^{2\beta} + 1} + 1 \right]$$

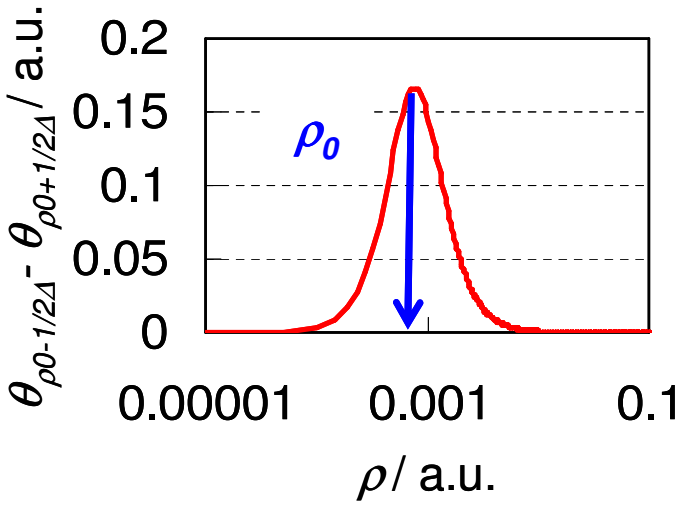

Method: Dispersion and repulsion free energies

Newly introduced term for periodic systems

Jinnouchi and Anderson, *PRB*, 77, 245417 (2008).

$$G_{ss,dr} + G_{ss,rep} = \sum_{\alpha} \left(a_{\alpha} S_{\alpha} + b_{\alpha} \right)$$

$$S_{\alpha} = \int \frac{p_{\alpha}(\mathbf{r} - \mathbf{R}_{\alpha})}{\sum_{\mathbf{R}} \sum_{\beta} p_{\beta}(\mathbf{r} - \mathbf{R}_{\beta} - \mathbf{R})} s[\rho_{AE}, \nabla \rho_{AE}] d\mathbf{r}$$

Partitioning function similar to that for numerical integration.

Partitioned atomic surface area

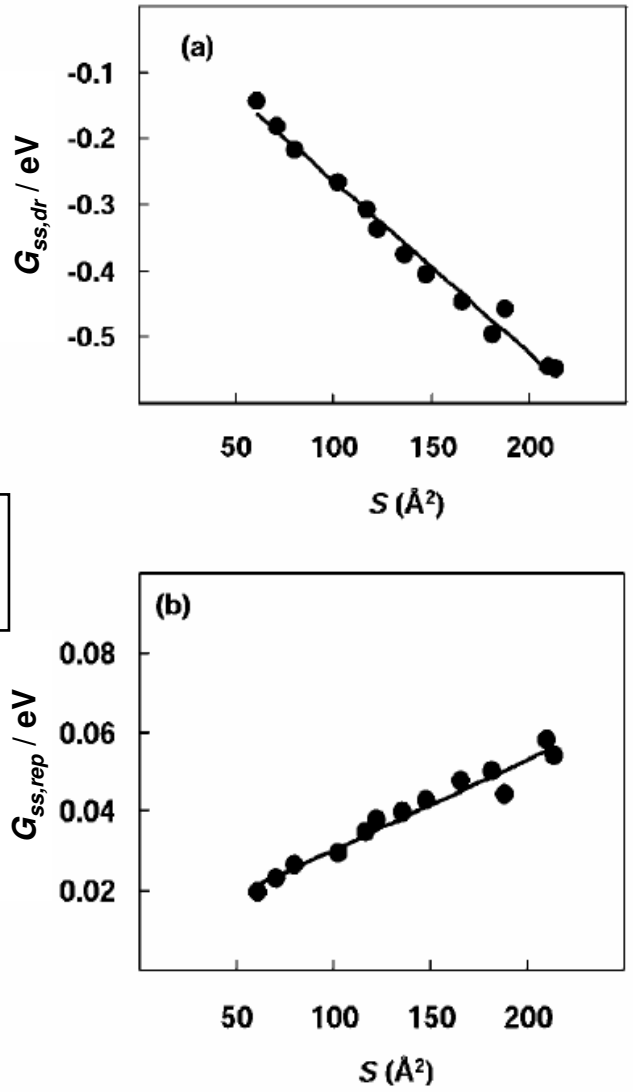

Method: non-electrostatic solute-ion interactions

Newly introduced term

Jinnouchi and Anderson, *PRB*, 77, 245417 (2008).

$$G_{is,nel} = \int d\mathbf{r}\left(\left|\rho_{-}(\mathbf{r})\right| + \left|\rho_{+}(\mathbf{r})\right|\right)\phi_{rep}(\mathbf{r})$$

$$\phi_{rep}(\mathbf{r}) = \sum_{\alpha=1}^{N}\sum_{\mathbf{R}} u\left(\left|\mathbf{r} - \mathbf{R}_{\alpha} - \mathbf{R}\right|\right)$$

The adaptive repulsive interaction term makes us possible to exclude ions in the MPB region from the DFT region in a consistent manner.

Method: energy minimization (1)

Variation with $\psi_i \rightarrow$ Kohn-Sham equation

$$\left[-\frac{1}{2}\nabla^2-\phi(\mathbf{r})+\sum_{\mathbf{R}}\sum_{\alpha}\left\{v_\alpha^{loc}\left(|\mathbf{r}-\mathbf{R}_\alpha-\mathbf{R}|\right)+\frac{Z_\alpha}{|\mathbf{r}-\mathbf{R}_\alpha-\mathbf{R}|}\right\}+\sum_{\mathbf{R}}\sum_{\alpha}\hat{V}_\alpha^{nl}+\frac{\delta E_{xc}^{GGA}}{\delta\rho}\right]\psi_i(\mathbf{r})=\varepsilon_i\psi_i(\mathbf{r})$$

Variation with $\phi \rightarrow$ Poisson equation

$$\nabla\varepsilon(\mathbf{r})\nabla\phi(\mathbf{r})=-4\pi\{-\rho(\mathbf{r})+\rho_+(\mathbf{r})-\rho_-(\mathbf{r})+\rho_c(\mathbf{r})\}$$

Variation with $\rho_\pm \rightarrow$ Modified Boltzmann distribution

$$\rho_\pm(\mathbf{r})=\frac{\frac{\phi_0}{2a^3}e^{\frac{\mp\phi(\mathbf{r})-\phi_{rep}(\mathbf{r})}{k_BT}}}{1-\phi_0+\phi_0\cosh\left(\frac{\phi(\mathbf{r})}{k_BT}\right)e^{\frac{-\phi_{rep}(\mathbf{r})}{k_BT}}}$$

The newly added repulsive potential for excluding the ions from the DFT region.

Method: energy minimization (2)

$$\nabla_{\mathbf{R}_\alpha} V = -\mathbf{F}_{HF} - \mathbf{F}_{Pulay} - \mathbf{F}_{solv,nonel}$$

$$\mathbf{F}_{HF} = -\int d\mathbf{r} \nabla_{\mathbf{R}_\alpha} \rho_c(\mathbf{r}) \phi(\mathbf{r})$$

Hellman-Feynman force

$$\mathbf{F}_{Pulay} = -\sum_{\sigma}\sum_{\mathbf{k}}\sum_{i}\int d\mathbf{r}[\nabla_{\mathbf{R}_\alpha}\psi^*_{i\mathbf{k}\sigma}(\mathbf{r})\left(\hat{H} - \varepsilon_{i\mathbf{k}\sigma}\right)\psi_{i\mathbf{k}\sigma}(\mathbf{r}) + \psi^*_{i\mathbf{k}\sigma}(\mathbf{r})\left(\hat{H} - \varepsilon_{i\mathbf{k}\sigma}\right)\nabla_{\mathbf{R}_\alpha}\psi_{i\mathbf{k}\sigma}(\mathbf{r})]$$

Pulay correction

$$\mathbf{F}_{solv,nonel} = \frac{1}{8\pi}\int d\mathbf{r}\nabla_{\mathbf{R}_\alpha}\rho_{AE}(\mathbf{r})\frac{d\varepsilon}{d\rho_{AE}}\left|\nabla\phi(\mathbf{r})\right|^2 - \int d\mathbf{r}\nabla_{\mathbf{R}_\alpha}\rho_{AE}(\mathbf{r})\frac{\delta G_{ss,nonel}}{\delta\rho_{AE}} - \int d\mathbf{r}\left(\left|\rho_-(\mathbf{r})\right| + \left|\rho_+(\mathbf{r})\right|\right)\nabla_{\mathbf{R}_\alpha}\phi_{rep}(\mathbf{r})$$

Non-electrostatic solvation force

Method: definition of the electrode potential

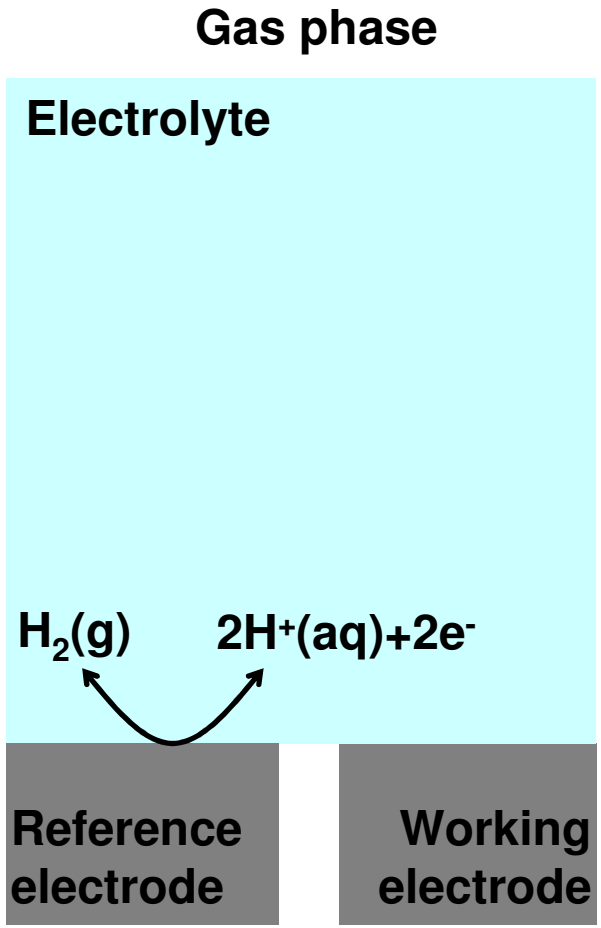

General equation

Electrode potential is obtained using work functions and free energies as follows,

$$U = -\frac{\mu - \phi_{\mathrm{SHE}}}{e}$$

$$\phi_{\mathrm{SHE}} = \frac{1}{2} G\left[\mathrm{H_2(g)}\right] - G\left[\mathrm{H^+(aq)}\right]$$

Method: definition of the electrode potential (2)

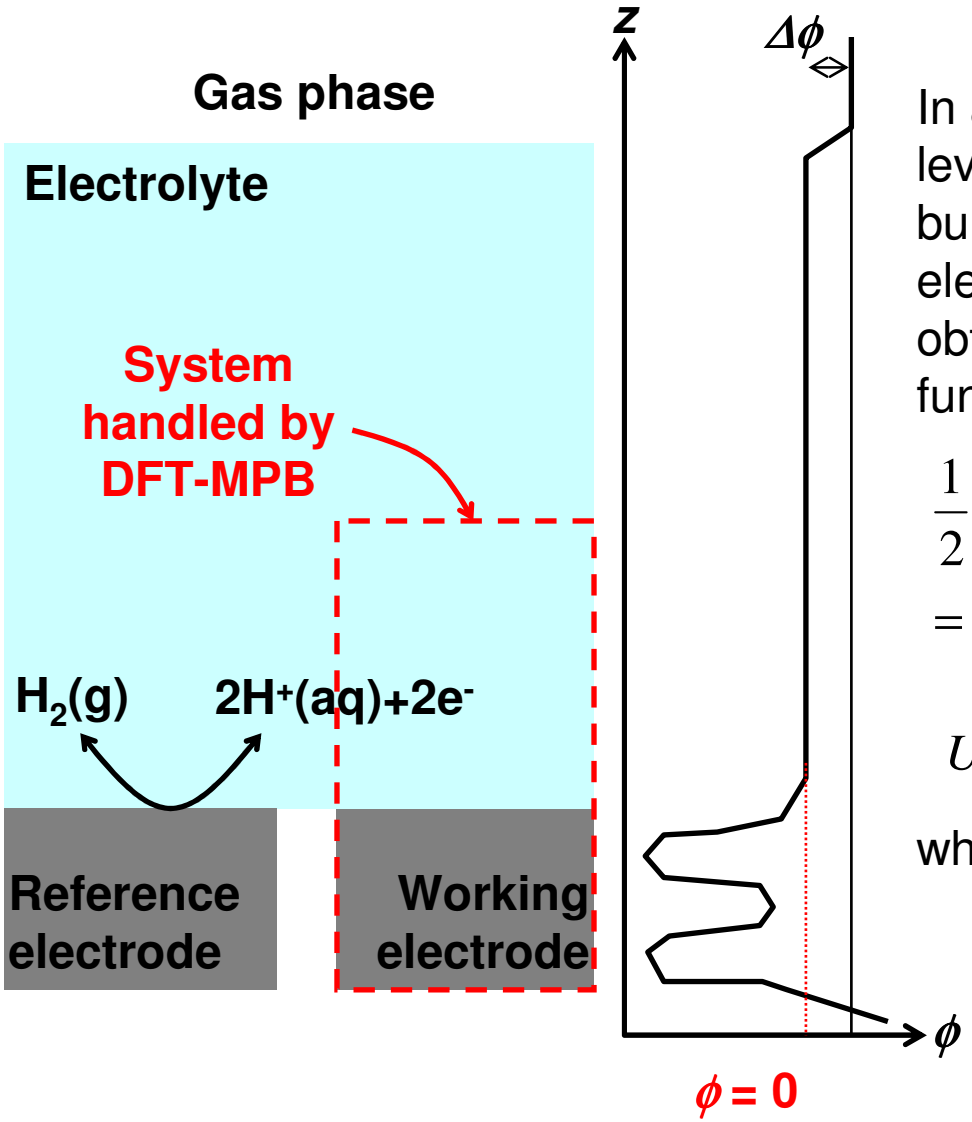

In actual computations, not the vacuum level but the electrostatic potential in the bulk MPB medium is set as zero. The electrode potential, however, can be exactly obtained by using the MPB scale work functions and free energies as follows,

$$\frac{1}{2}G[\mathrm{H_2(g)}] = (\phi'_{\mathrm{SHE}} + \cancel{\Delta\phi}) + (G'[\mathrm{H^+(aq)}] - \cancel{\Delta\phi})$$

$$= \phi'_{\mathrm{SHE}} + G'[\mathrm{H^+(aq)}]$$

$$U = -\frac{\mu' - \phi'_{\mathrm{SHE}}}{e}$$

where prime indicates the MPB scale.

Method: well-defined electrostatic potential at bulk electrolyte

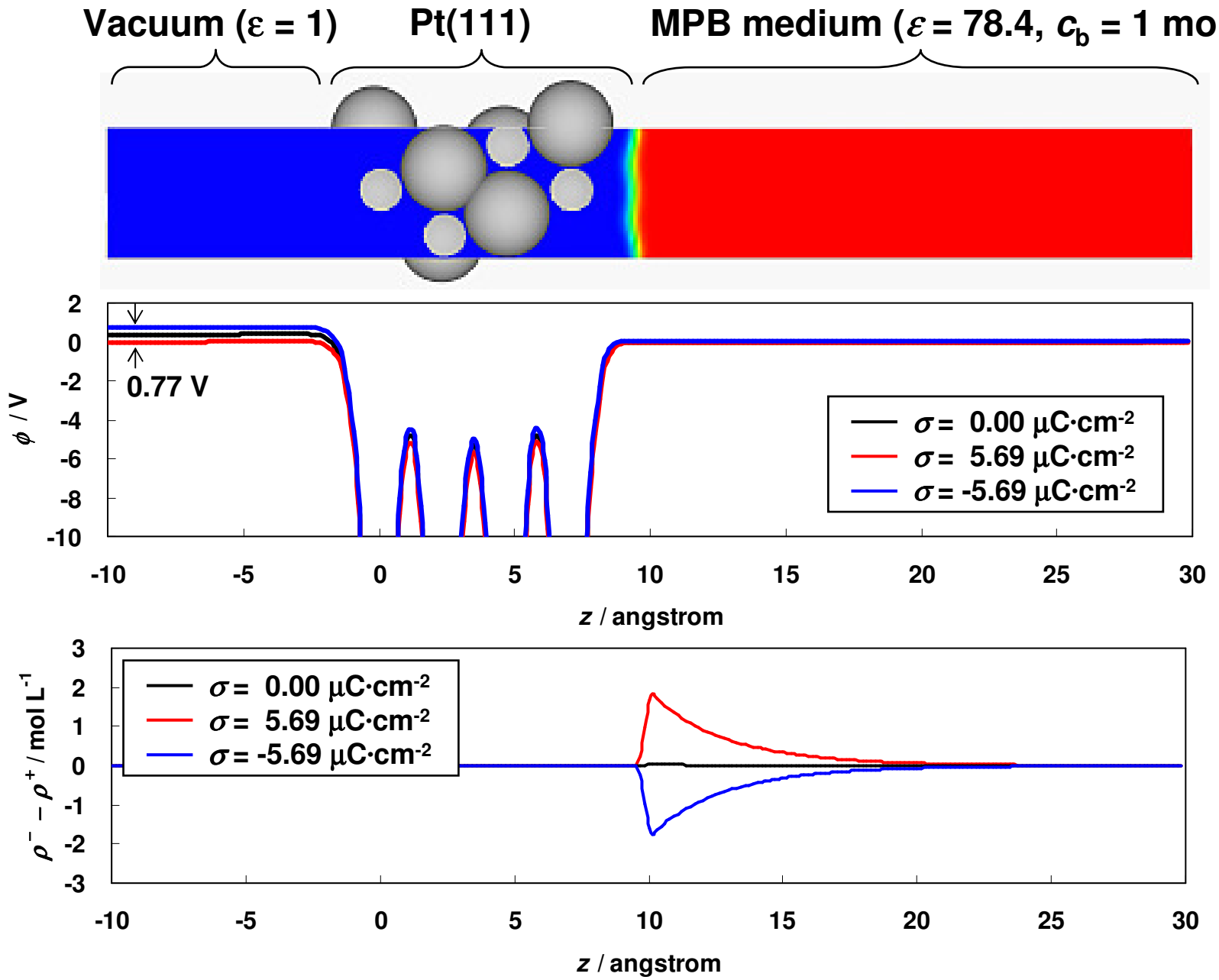

Method: implementation (1)

All those methodologies are implemented in a home-made DFT code which uses

- **LCPAOs as basis set,**
- **relativistic norm-conserving pseudopotentials as effective core potentials,**
- **atom centered Lebedev grid for numerical integration,**
- **system with and without 2-dimensional or 3-dimensional periodic boundary condition.**

Method: implementation (2)

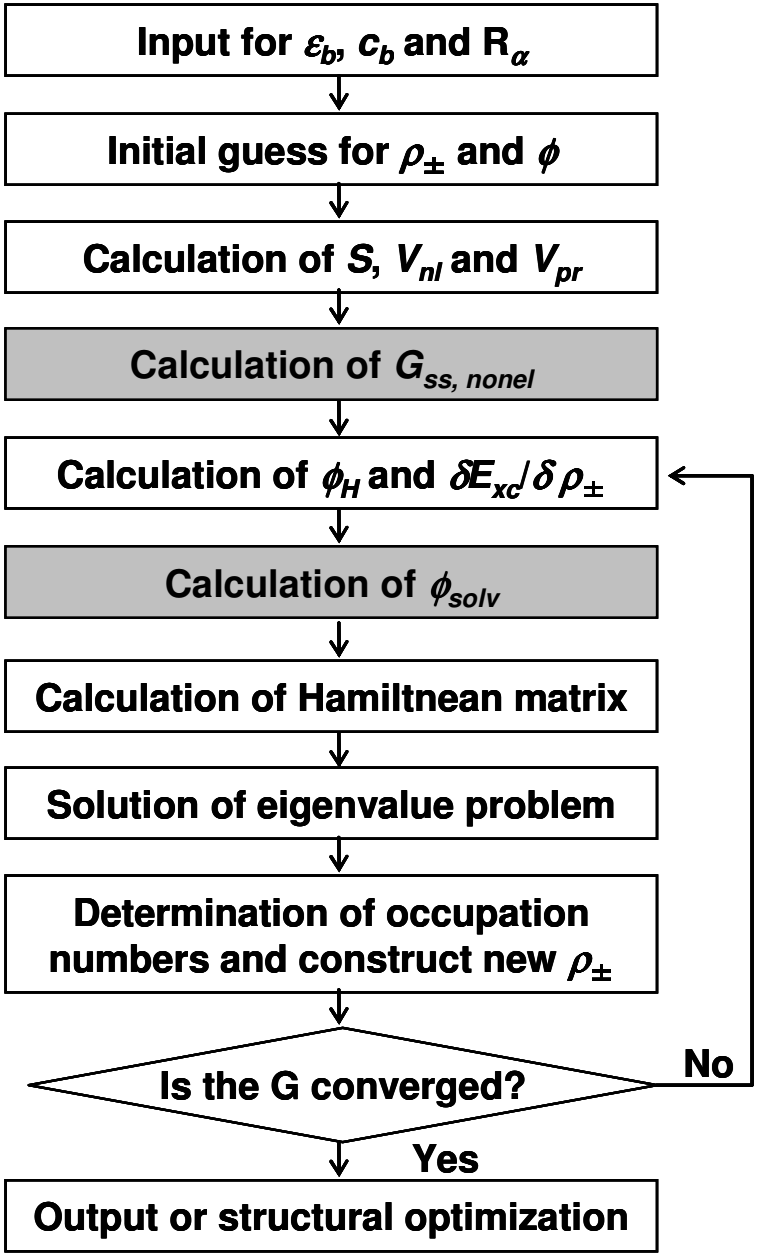

The subroutine on the calculation of electrostatic potential in vacuum is simply replaced by the subroutine on the calculation of electrostatic potential in MPB medium.

Method: implementation (3)

No PBC

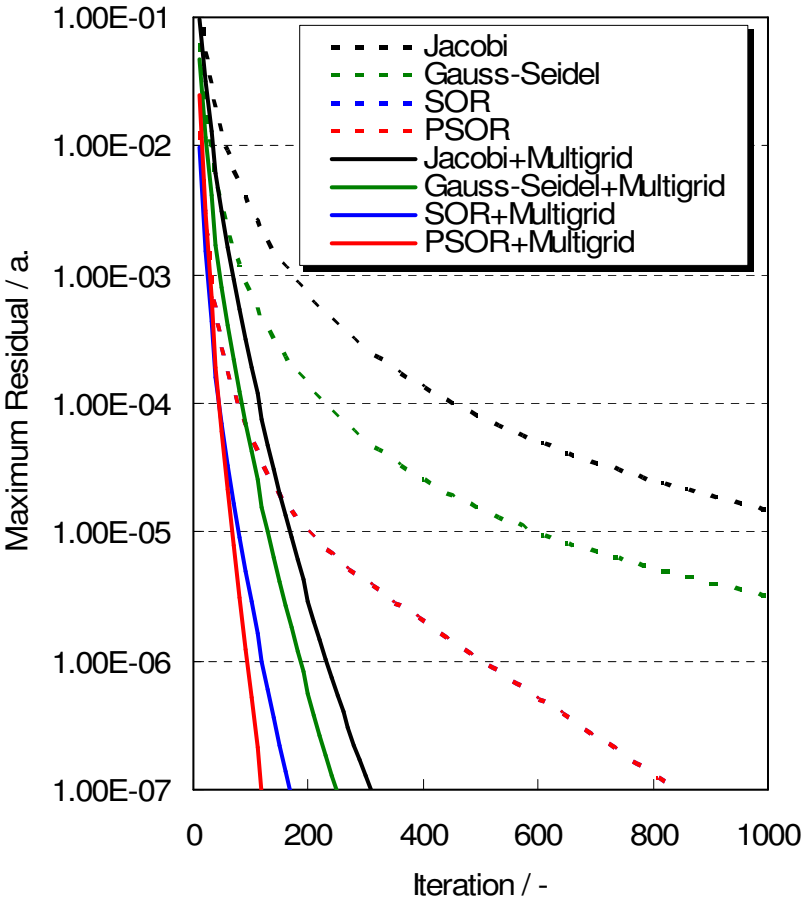

2D-PBC

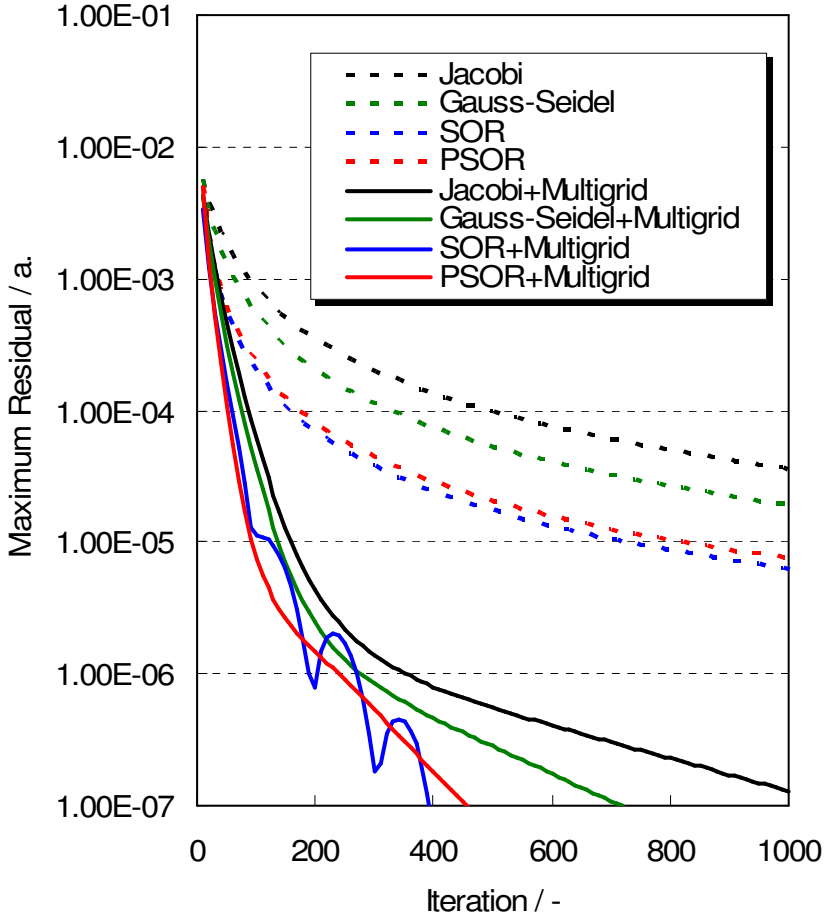

PSOR+Multigrid: Good convergence & Parallelization OK

Method: problems and practical calculations

We currently do not execute MD using DFT-MPB because of following reasons.

(i) MD without constraining *U* does not give information comparable with experiments. MD with constraining *U* is (was) difficult.

(ii) Simpler analysis using model chemistry sometimes give very useful information on the mechanism.

(iii) The simple model is definitely necessary in practical designning of electrocatalysts.

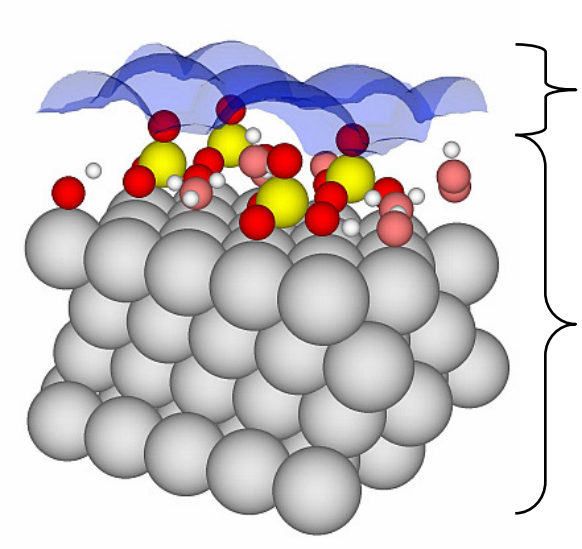

Molecules on top of the solvation shell are assumed to be bulk like and handled by continuum solvation model.

Surface and molecules in the first (or second) solvation shell is assumed to be rigidly bounded to the surface and handled by DFT. Free energy contributions by those atomic motions are estimated by integrating simple partition functions.

After checking energies of several possible structures, the minimum one is chosen as the explicit molecular model.

41

Method: approximations in Gibbs free energies

$$G = -k_B T \ln \int e^{-\frac{\sum_\alpha \frac{|\mathbf{P}_\alpha|^2}{2M_\alpha} + V(\{\mathbf{R}_\alpha\}) + pV}{k_B T}} \prod_\alpha d\mathbf{P}_\alpha d\mathbf{R}_\alpha dV$$

Approximation:

Integrations using simple models with translation and rotation of rigid body and harmonic vibrations.

$$G \cong V\left(\left\{\mathbf{R}_\alpha^0\right\}\right) + H_n - TS_n$$

Application 1: aqueous and surface redox potentials

Application 1: aqueous and surface redox potentials

Application of our new theory, which can seamlessly connect bulk solution phases to liquid-solid interfacial phases, to aqueous and surface redox potentials

(i) to clarify the surface effects on the redox potentials

(ii) and to check the accuracy of our new theory.

Application: aqueous and surface redox potentials

Computational parameters

XC:	GGA-PBE or GGA-RPBE
Basis set:	Double zeta plus polarization with cutoff radius of 8.0 bohr.
PPs:	Troullier-Martins type scalar relativistic pseudopotentials.
Model:	Isolated molecules and ions without PBC Slabs with 2D-PBC of $2\times\sqrt{3}$ or $3\times\sqrt{3}$.

$H^+(H_2O)_4$ (aq)

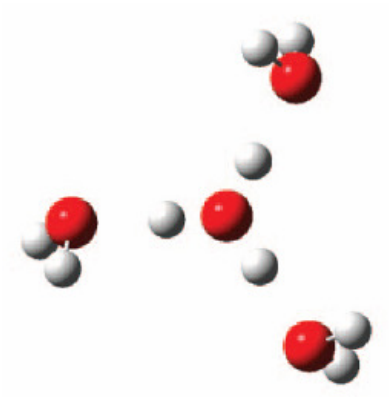

$(HO_2+H_2O)/Pt(111)$

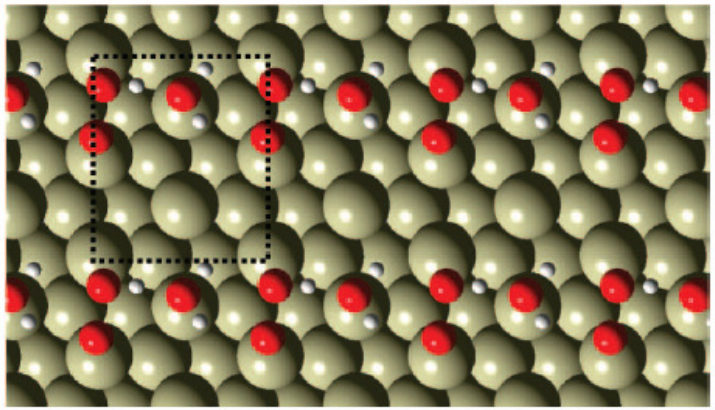

Jinnouchi and Anderson, *J. Phys. Chem. C*, 112, 8747 (2008).

Application: solvation free energies

Reaction free energy of $A(g) + (H_2O)_n(aq) \rightarrow A(H_2O)_n(aq)$.

Chemical specie	GGA-PBE	GGA-RPBE	PBEPBE in G03	Exp.
$H^+(aq)$	-11.36	-11.39	-11.59	-11.379
$OH^-(aq)$	-4.98	-4.82	-4.45	-4.64
$O_2^-(aq)$	-3.66	-3.58	-3.43	-3.69
$HO_2^-(aq)$	-4.19	-4.28	-4.01	-4.29
$Cl^-(aq)$	-3.24	-3.36	-3.15	-3.17
$F^-(aq)$	-	-4.18	-3.82	-4.42
$Br^-(aq)$	-	-3.13	-2.83	-3.15
$H_2O(aq)$	-0.24	-0.09	-0.24	-0.27
$H_2O_2(aq)$	-0.28	-0.22	-0.23	-0.38
$HClO(aq)$	-0.19	-0.11	-	-0.08
$HClO_2(aq)$	-0.29	-0.23	-	-

Unit is eV.

Fitting only one parameter ρ_0 is enough to reproduce the solvation free energies accurately.
The accuracy is similar to that of PCM in Gaussian03.

Jinnouchi and Anderson, *J. Phys. Chem. C*, 112, 8747 (2008).

Application: aqueous redox potentials (1)

TABLE 1: Aqueous Redox Potentials from Theories and Experiments

reactions	PBE	RPBE	exp.[a]
O_2 (g) + H^+ (aq) + e^- ↔ O (g) + OH (g)	−3.35	−3.08	−2.76
H^+ (aq) + e^- ↔ H (g)	−1.98	−2.00	−2.11
H_2O (aq) + e^- ↔ $^1/_2H_2$ (g) + OH^- (aq)	−0.71	−0.73	−0.83
O_2 (g) + e^- ↔ O_2^- (aq)	−0.37	−0.65	−0.33
HO_2^- (aq) + H_2O (aq) + e^- ↔ OH (g) + $2OH^-$ (aq)	−0.09	−0.13	−0.25
$^1/_2O_2$ (g) + H_2O (aq) + e^- ↔ $^1/_2H_2O_2$ (aq) + OH^- (aq)	−0.16	−0.33	−0.13
H_2O_2 (aq) + e^- ↔ OH (g) + OH^- (aq)	−0.17	−0.11	−0.11
$^1/_2O_2$ (g) + $^1/_2H_2O$ (aq) + e^- ↔ $^1/_2OH^-$ (aq) + $^1/_2HO_2^-$ (aq)	−0.20	−0.32	−0.06
O_2 (aq) + H^+ (aq) + e^- ↔ HO_2 (aq)	0.00	−0.25	−0.05
H^+ (aq) + e^- ↔ $^1/_2H_2$ (g)	0.00	0.00	0.00
O_2^- (aq) + H_2O (aq) + e^- ↔ HO_2^- (aq) + OH^- (aq)	−0.03	0.00	0.20
O_2 (g) + H^+ (aq) + e^- ↔ $^1/_2O_3$ (g) + $^1/_2H_2O$ (aq)	0.28	0.06	0.38
$^1/_4O_2$ (g) + $^1/_2H_2O$ (aq) + e^- ↔ OH^- (aq)	0.40	0.24	0.42
O_3 (g) + H_2O (aq) + e^- ↔ O_2 (g) + OH (g) + OH^- (aq)	0.37	0.55	0.51
$^1/_3O_2^-$ (aq) + $^2/_3H_2O$ (aq) + e^- ↔ $^4/_3OH^-$ (aq)	0.65	0.53	0.64
$^1/_2O_2$ (g) + H^+ (aq) + e^- ↔ $^1/_2H_2O_2$ (aq)	0.55	0.39	0.70
H_2O_2 (aq) + H^+ (aq) + e^- ↔ OH (g) + H_2O (aq)	0.54	0.62	0.71
HO_2 (aq) + e^- ↔ HO_2^- (aq)	0.31	0.33	0.74
HO_2 (aq) + O_2 (g) + H^+ (aq) + e^- ↔ O_3 (g) + H_2O (aq)	0.56	0.38	0.81
$^1/_2HO_2^-$ (aq) + $^1/_2H_2O$ (aq) + e^- ↔ $^3/_2OH^-$ (aq)	0.99	0.80	0.87
$^1/_2H_2O_2$ (aq) + e^- ↔ OH^- (g)	0.95	0.81	0.93
$^1/_2HO_2$ (aq) + H^+ (aq) + e^- ↔ $^1/_2OH$ (g) + $^1/_2H_2O$ (aq)	0.82	0.83	1.07
$^1/_4O_2$ (g) + H^+ (aq) + e^- ↔ $^1/_2H_2O$ (g)	1.08	1.01	1.23
$^1/_2O_3$ (g) + $^1/_2H_2O$ (aq) + e^- ↔ $^1/_2O_2$ (g) + OH^- (aq)	1.22	1.14	1.24
O_3 (g) + H^+ (aq) + e^- ↔ O_2 (g) + OH (g)	1.08	1.28	1.34
$^1/_2Cl_2$ (g) + e^- ↔ Cl^- (aq)	1.26	1.21	1.36
HO_2 (aq) + H^+ (aq) + e^- ↔ H_2O_2 (aq)	1.34	1.14	1.44
$^1/_4HClO_2$ (aq) + $^3/_4H^+$ (aq) + e^- ↔ $^1/_4Cl^-$ (aq) + $^1/_2H_2O$ (aq)	1.58	1.51	1.58
HClO (aq) + H^+ (aq) + e^- ↔ $^1/_2Cl_2$ (g) + H_2O (aq)	1.58	1.50	1.63
$^1/_3HO_2$ (aq) + H^+ (aq) + e^- ↔ $^2/_3H_2O$ (aq)	1.48	1.37	1.65
$^1/_2H_2O_2$ (aq) + H^+ (aq) + e^- ↔ H_2O (aq)	1.66	1.54	1.76
$^1/_3HClO_2$ (aq) + H^+ (aq) + e^- ↔ $^1/_6Cl_2$ (g) + $^2/_3H_2O$ (aq)	1.68	1.61	1.66
OH (g) + e^- ↔ OH^- (aq)	2.08	1.72	1.98
OH (g) + H^+ (aq) + e^- ↔ H_2O (aq)	2.96	2.45	2.81
mean absolute error	0.13	0.19	

Jinnouchi and Anderson, *J. Phys. Chem. C*, 112, 8747 (2008).

Application: aqueous redox potentials (2)

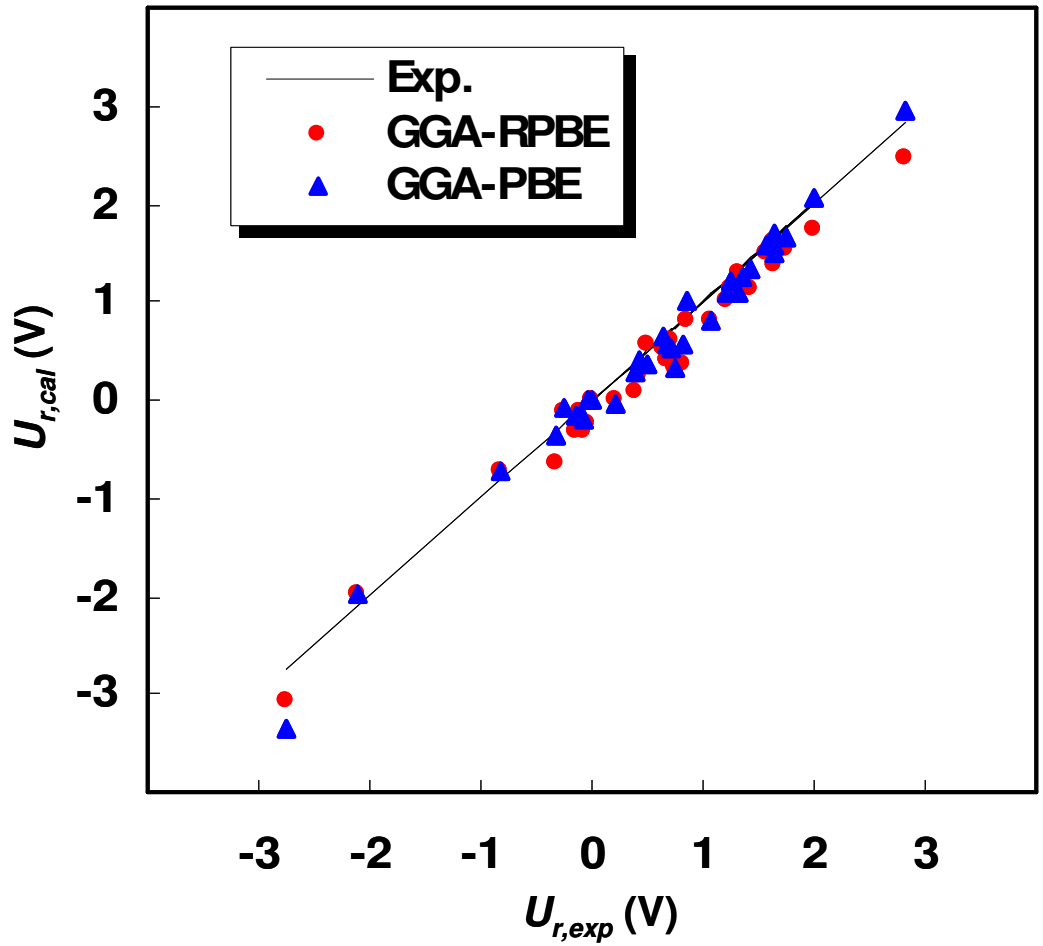

Total 34 aqueous redox potentials are reproduced within an average errors of 0.13 V and 0.19 eV by GGA-PBE and GGA-RPBE, respectively.

Jinnouchi and Anderson, *J. Phys. Chem. C*, 112, 8747 (2008).

Application: surface redox potentials (1)

Reaction	PBE	RPBE	Exp.
$H^+(aq) + e^- \leftrightarrow H(ads)$ ($\theta = 1/4$)	0.31	0.27	0.32
$OH(ads) + H^+(aq) + e^- \leftrightarrow H_2O(ads)$ ($\theta = 1/3$)	0.40	0.51	0.68
$O(ads) + H^+(aq) + e^- \leftrightarrow OH(ads)$ ($\theta = 1/4$)	1.42	1.12	≈1.0
$O_2(g) + H^+(aq) + e^- \leftrightarrow HO_2(ads)$ ($\theta = 1/4$)	0.82	0.34	-
Average error	0.29	0.13	-

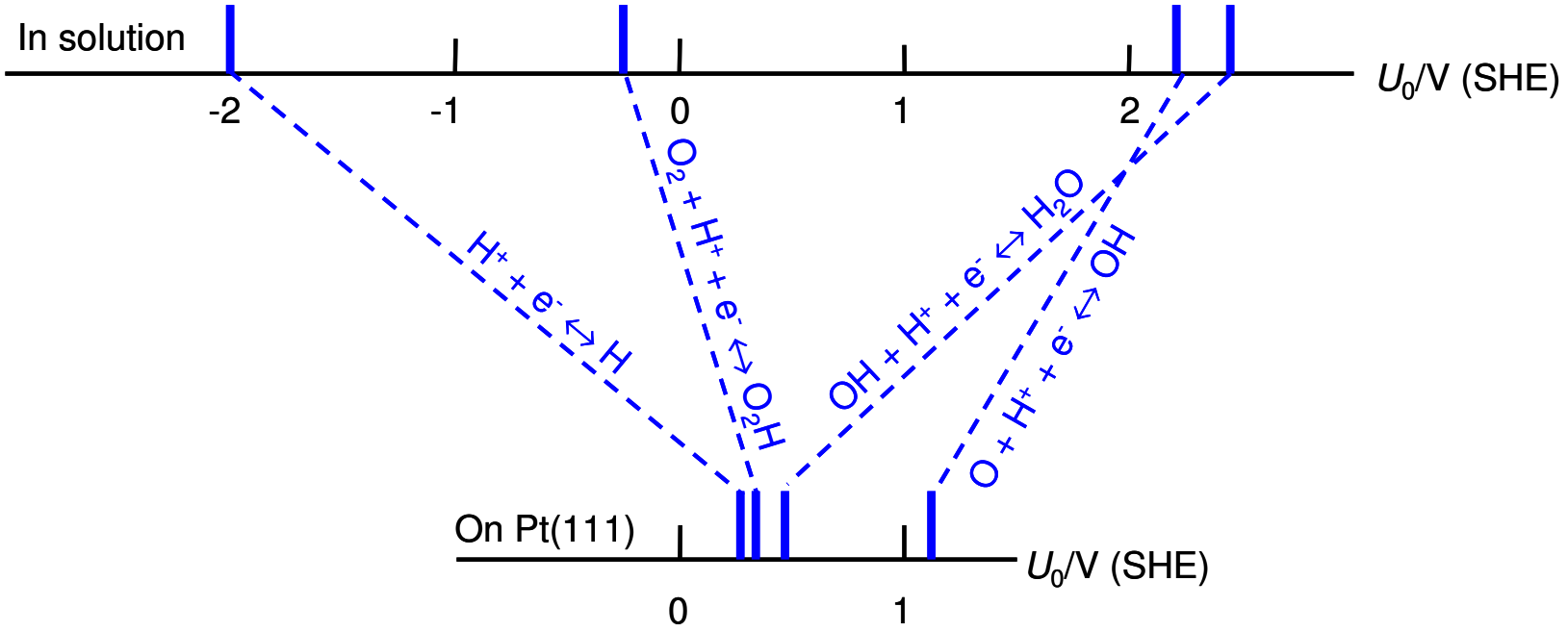

Jinnouchi and Anderson, *J. Phys. Chem. C*, 112, 8747 (2008).

Application: surface redox potentials (2)

Contributions by thermal corrections on atomic motions, solvation free energies and surface charging on surface redox potentials.

$-(\Delta H_{corr}-T\Delta S_{corr})$	$-\Delta G_{solv}/nF$	$-\Delta G_{sc}/nF$
Contributions by thermal corrections on atomic motions	Contributions by solvation free energies	Contributions by surface charging
0.35	0.37	0.07

Contributions by the surface charging is small (±0.07 V) for redox potentials of H(ads), OH(ads) and O(ads) formations.

This is why methodologies using neutral slabs suggested by Anderson's group and Nørskov's group work well.

Jinnouchi and Anderson, *J. Phys. Chem. C*, 112, 8747 (2008).

Application: conclusion

(i) Solvation free energies are in good agreement with experiments.

(ii) Both aqueous and surface redox potentials also are in good agreement with experiments.

(iii) RPBE gives more accurate surface redox potentials than PBE does due to more accurate descriptions of binding energies between adsorbates and the surface.

(iv) Effects of surface charging on the surface redox potentials of H(ads), OH(ads) and O(ads) are ±0.07 V. Hence, methodologies using neutral slabs can reasonably predict those redox potentials.

Application: PZC and roles of the dielectric medium

Jinnouchi and Anderson, *PRB*, 77, 245417 (2008).

Fundamental questions on the dielectric medium:

(i) what is the role of the dielectric medium?

(ii) how does PZC change by changing the water model?

Application: model

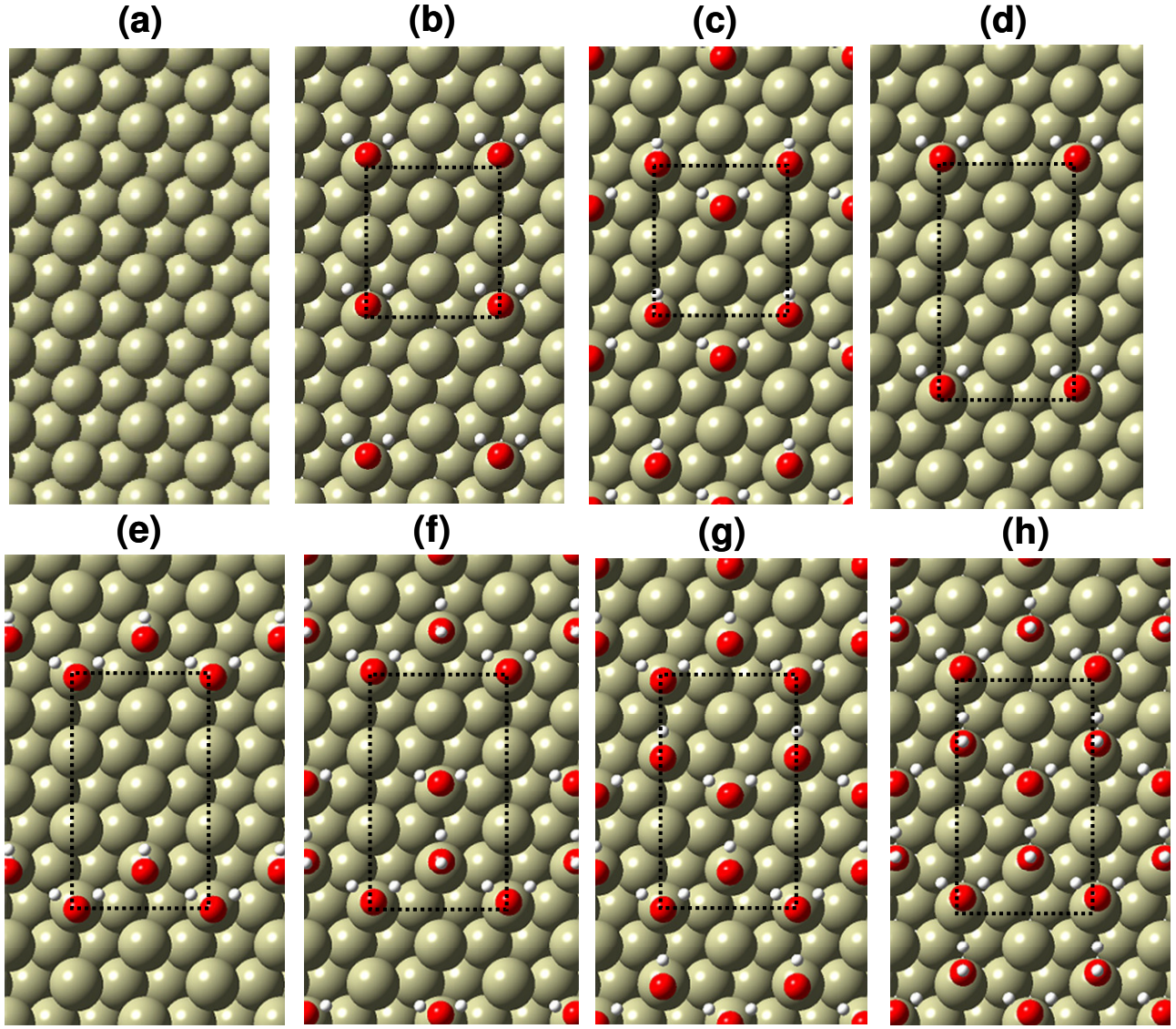

Jinnouchi and Anderson, *PRB*, 77, 245417 (2008).

Application: PZC without the dielectric medium

Jinnouchi and Anderson, *PRB*, 77, 245417 (2008).

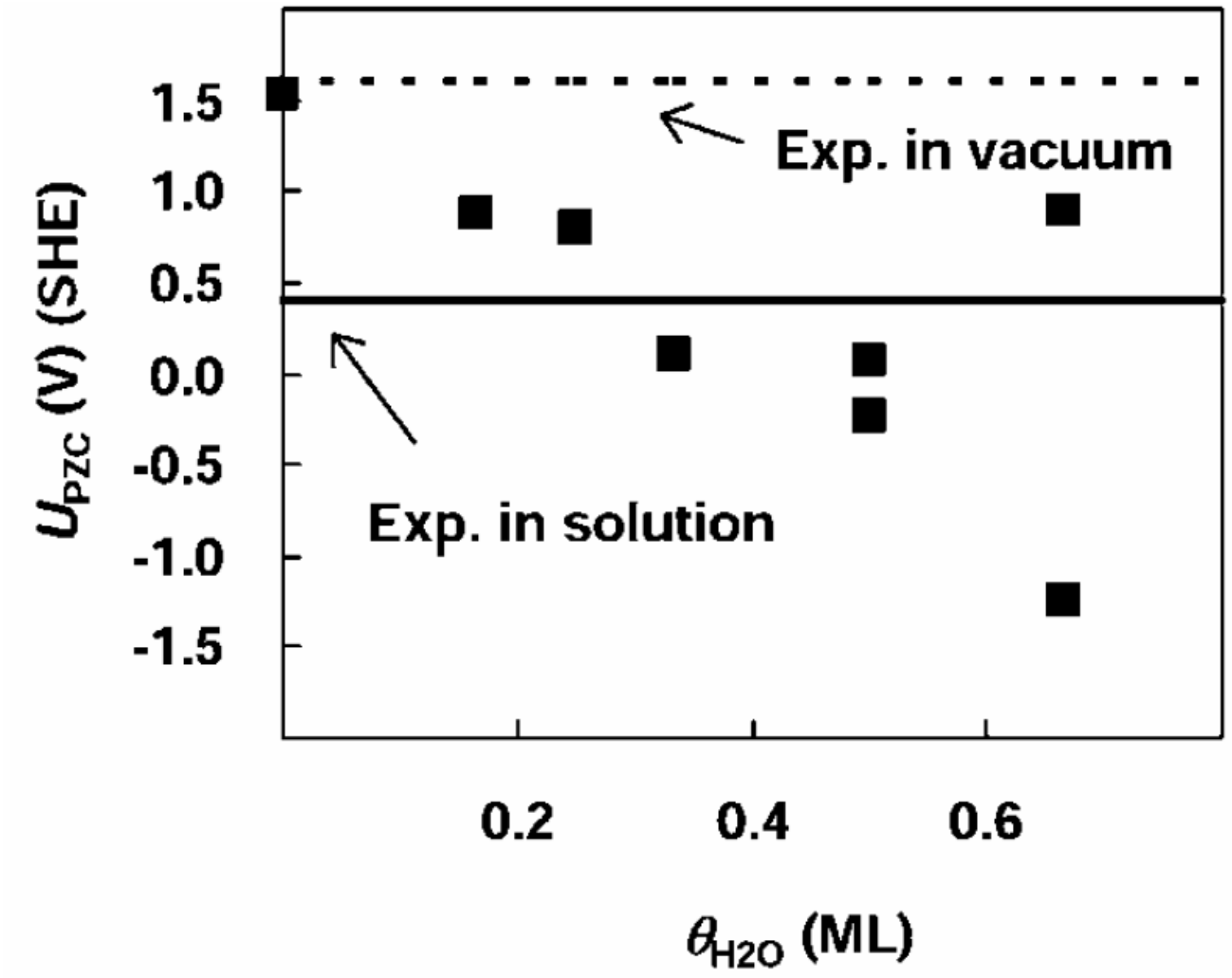

PZC (work function) largely fluctuates with the change in the surface coverage of water.

Application: the reason for the fluctuations (1)

Jinnouchi and Anderson, *PRB*, 77, 245417 (2008).

The change in the dipole moment normal to the surface can be decomposed into a contribution by the water orientation and contribution by the interfacial polarization due to the adsorption.

$$\Delta\phi_{dip} = -\frac{4\pi}{S}\int d\mathbf{r}\left(\rho(\mathbf{r})+\rho_c(\mathbf{r})\right)z = \Delta\phi_{dip,ori} + \Delta\phi_{dip,pol}$$

Dipole moment of the water orientation given by the dipole moment of isolated water layer.

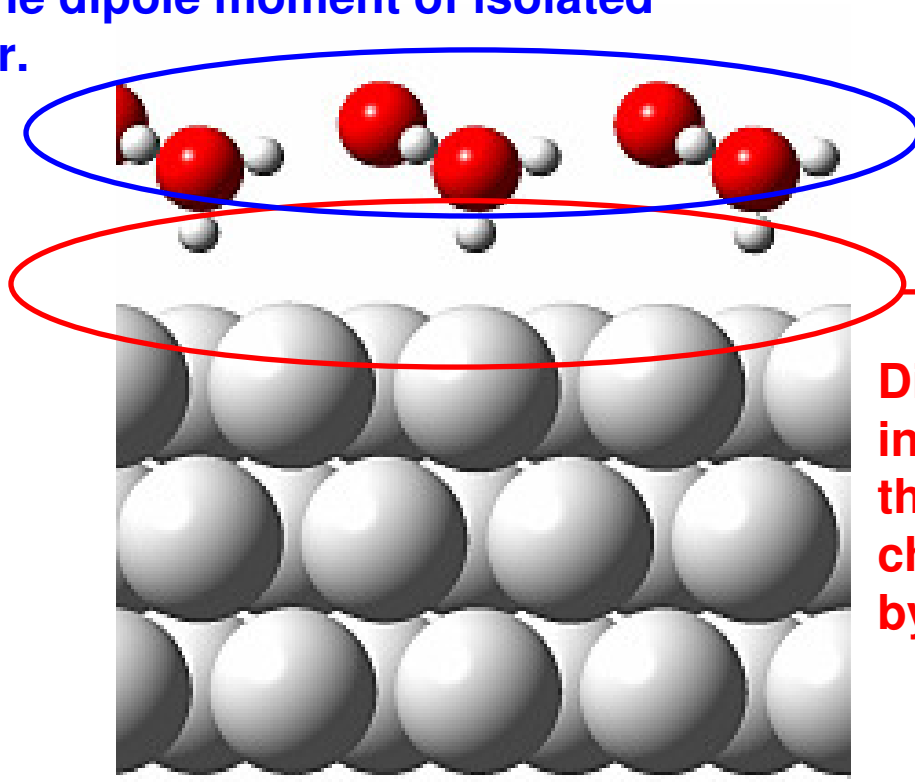

Dipole moment by the interfacial polarization due to the adsorption given by the change in the electron density by the adsorption.

Application: the reason for the fluctuations (2)

Jinnouchi and Anderson, *PRB*, 77, 245417 (2008).

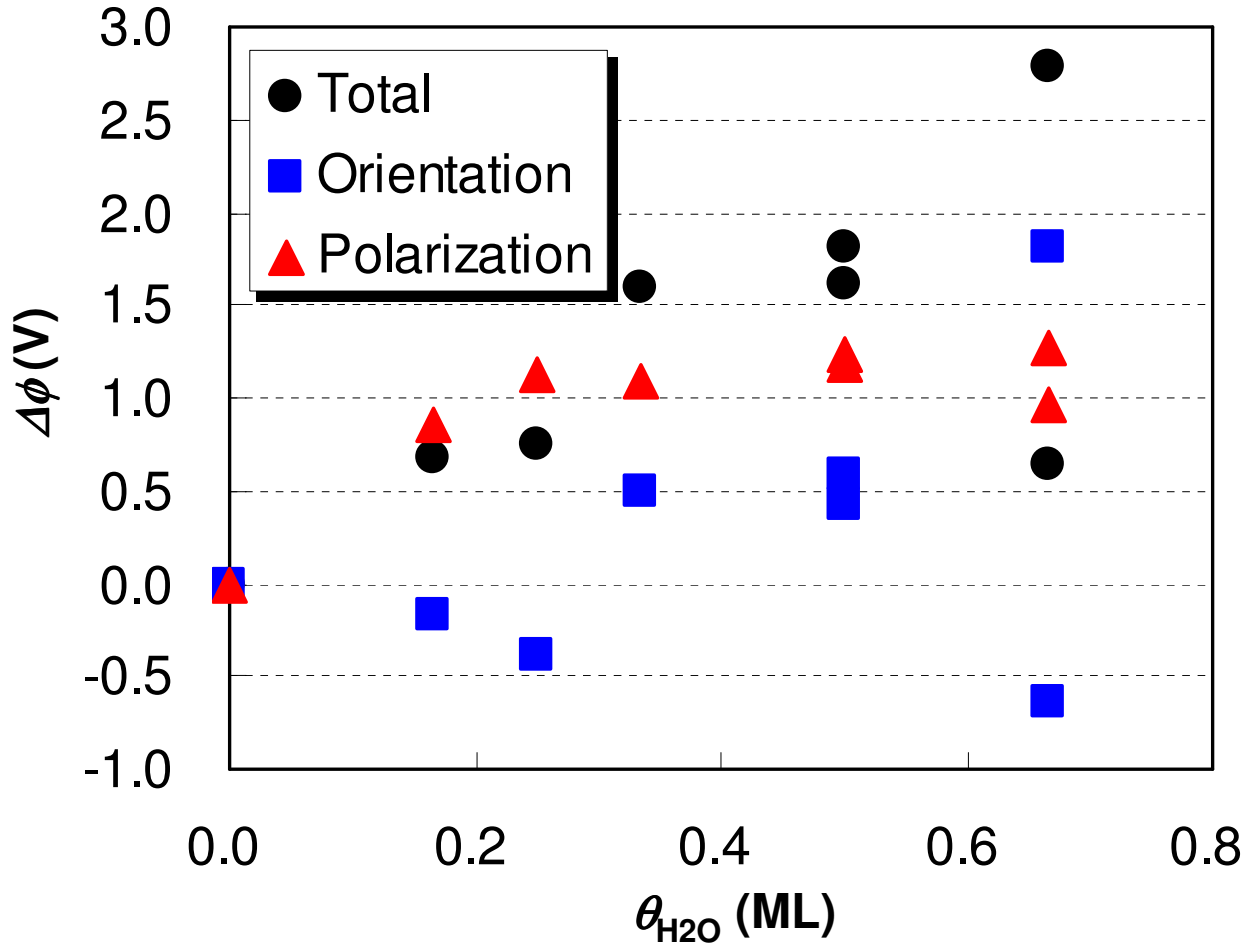

The fluctuations stem from the fluctuations in the dipole moment by the water orientation.

Application: the polarization contribution dominates PZC?

Jinnouchi and Anderson, *PRB*, 77, 245417 (2008).

Eliminating orientation contribution

$$U'_{PZC} = -\frac{(\mu - e\Delta\phi_{ori}) - \phi_{\mathrm{SHE}}}{e} = U_{PZC} + \Delta\phi_{ori}$$

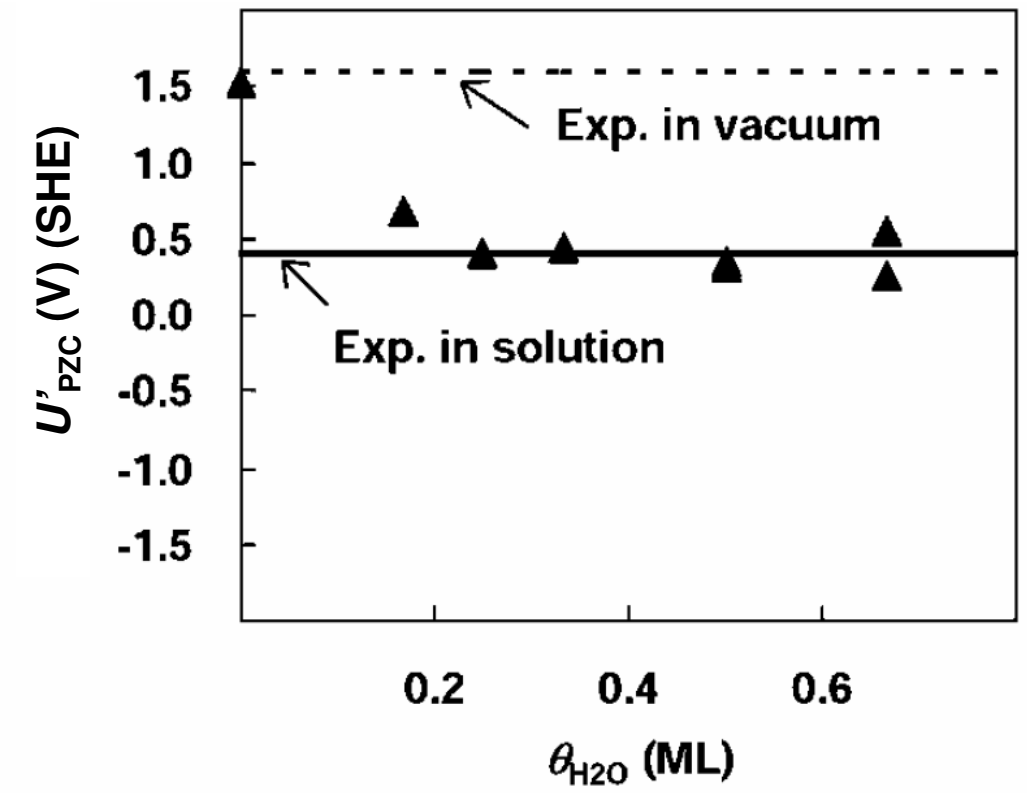

By eliminating the orientation contribution, calculated PZC becomes closer to the experimental PZC.

Application: PZC with the dielectric medium

Jinnouchi and Anderson, *PRB*, 77, 245417 (2008).

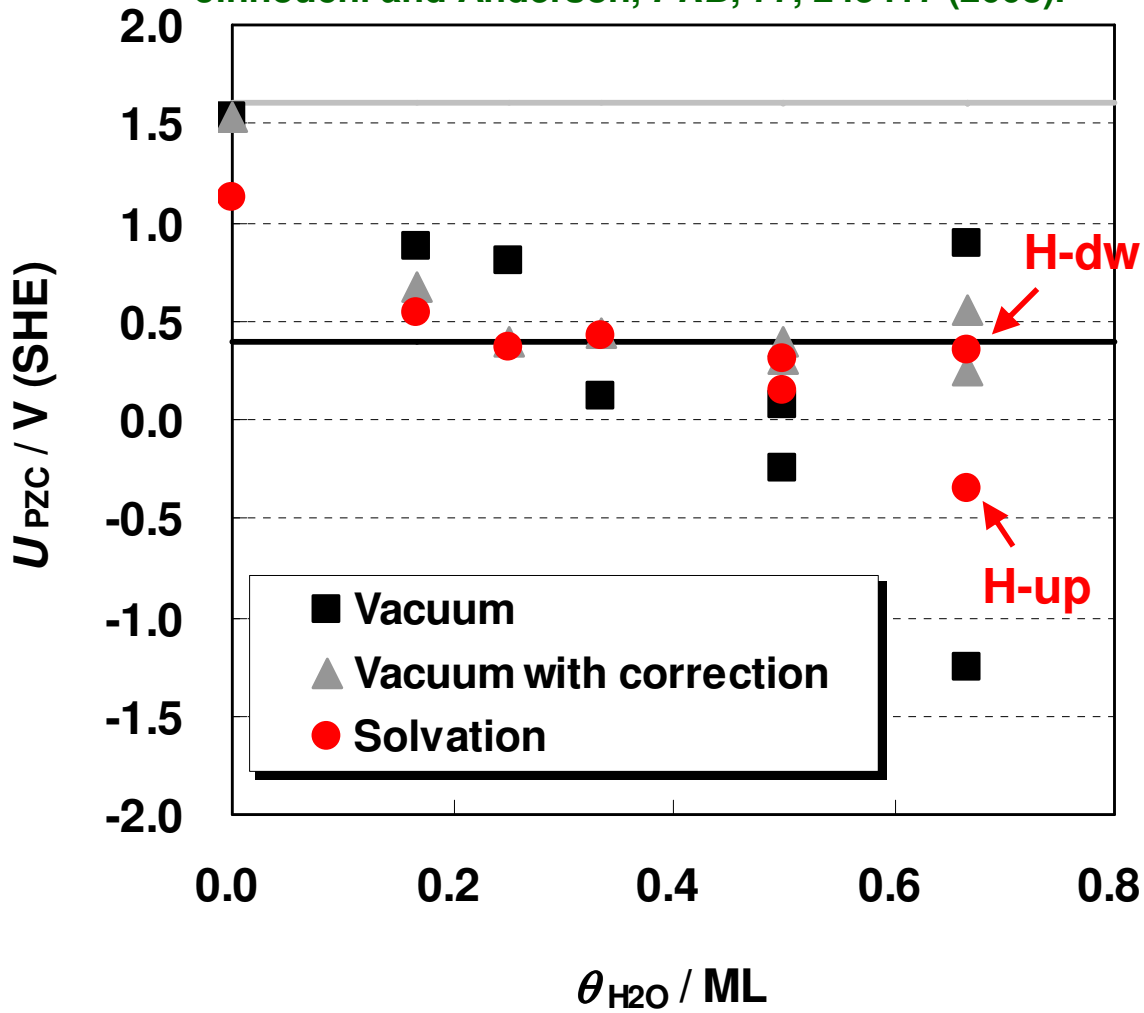

The dielectric medium reduces the fluctuation, but the fluctuation still remains. An actual interfacial water orientation at PZC is probably a mixture of H-up and H-down structures, and therefore, PZC becomes an average of PZCs of those structures.

Application: fitting cavity size to reproduce PZC

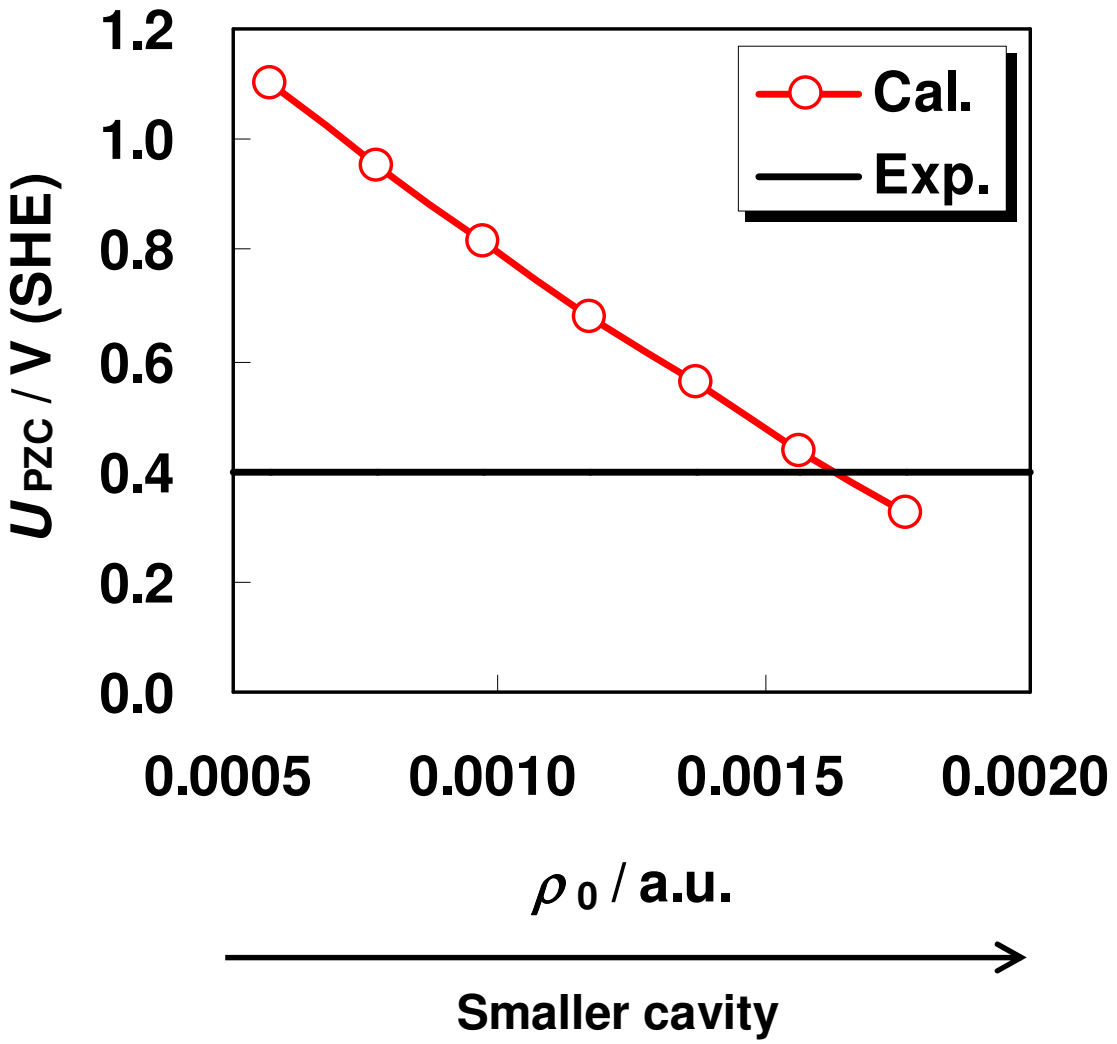

The experimental PZC can be obtained by fitting solvation parameters to decrease the cavity size.

Application: role of the dielectric medium

Qualitatively right direction of the solvation

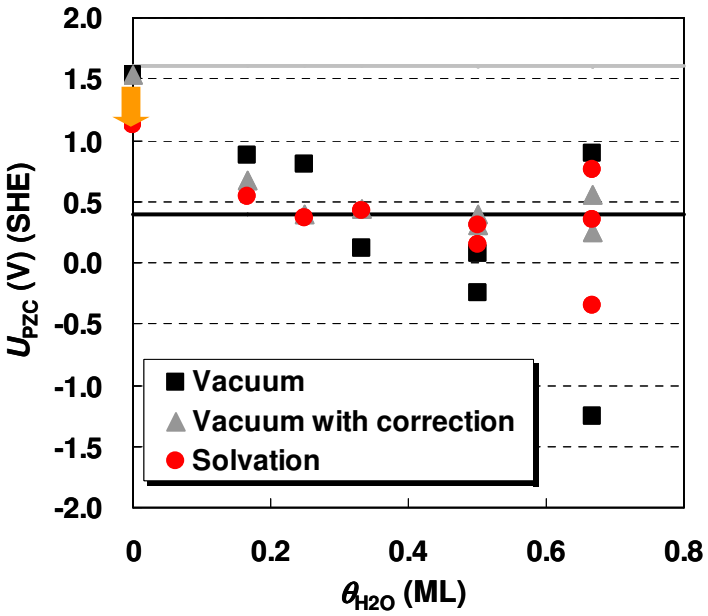

The effect of the dielectric medium can be visualized by analyzing a following equivalent charge distribution change.

$$\Delta\rho_\varepsilon(\mathbf{r}) = \rho_\varepsilon(\mathbf{r}) - \rho(\mathbf{r})$$

$$\rho_\varepsilon(\mathbf{r}) = \frac{\rho_e(\mathbf{r}) + \rho_c(\mathbf{r}) + \rho_+(\mathbf{r}) + \rho_-(\mathbf{r})}{\sqrt{\varepsilon(\mathbf{r})}} - \frac{1}{4\pi}\nabla^2\sqrt{\varepsilon(\mathbf{r})}\phi(\mathbf{r})$$

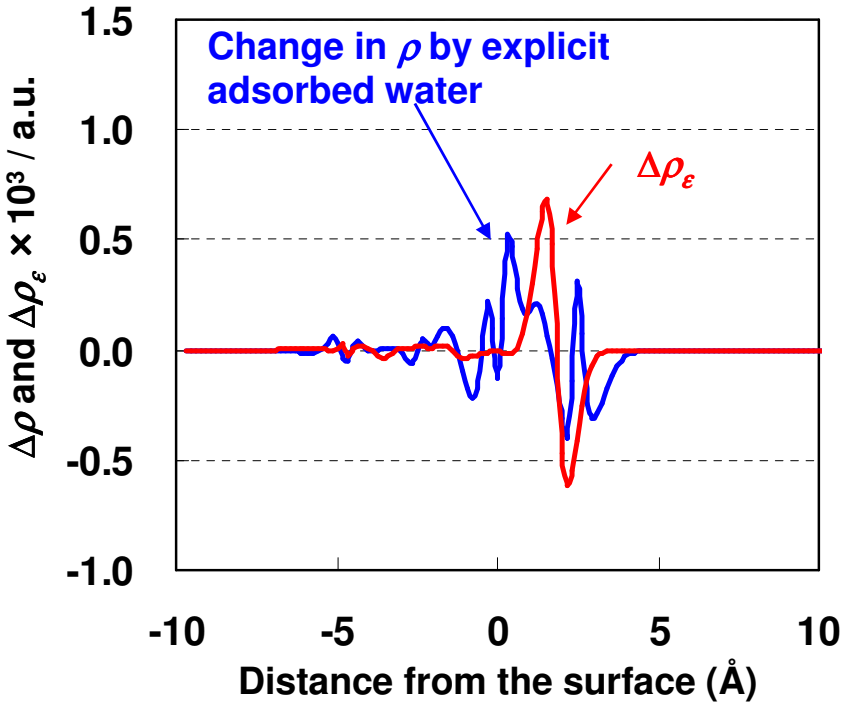

The dielectric medium gives a polarization similar to that by the actual water adsorptions. Decreasing the cavity size causes larger polarization.

Application: conclusion

(i) The work function of the slab covered by water in vacuum largely fluctuates by fluctuations in the dipole moment caused by the water orientations.

(ii) By eliminating the potential gap due to the water orientations from the work function, the result becomes closer to the experimental result.

(iii) The dielectric medium reduces the fluctuations in the PZC.

(iv) The dielectric medium gives a polarization similar to that caused by the actual water adsorption.

Concluding remarks

A new theory combining DFT with MPB was developed.

The theory can be applied to both bulk solution reactions and liquid-solid interfacial reactions and gives aqueous and surface redox potentials within a practically useful accuracy.

We believed that the new theory find many applications in the field of electrocatalysis in 2008, and it actually gives very useful information now as will be shown in the next presentation.

Acknowledgement

This work was supported by Toyota Central R&D Labs., Inc. and by a Multi-University Research-Initiative (MURI) Grant No. DAAD19-03-1-0169 from the U.S. Army Research Office to Case Western Reserve University.